Food Hydrocolloids 166 (2025) 111316

Contents lists available at ScienceDirect

Food Hydrocolloids

journal homepage: www.elsevier.com/locate/foodhyd

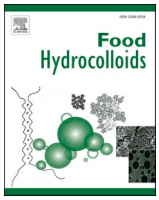

Zein/chitosan/cellulose nanocrystal based active food contact layer: Unlocking the interrelations between release behavior, mechanical stability, and hydrolysis

Lucie Pavlatkova [a,b,1], Ece Sogut [a,c,1], Jana Sedlarikova [d], Pavel Pleva [b], Lucas Petit [e], Milan Masar [f], Petra Peer [b], Magda Janalikova [b,*], Ilke Uysal-Unalan [a,g,**]

[a] Department of Food Science, Aarhus University, Agro Food Park 48, 8200, Aarhus N, Denmark
[b] Department of Environmental Protection Engineering, Faculty of Technology, Tomas Bata University in Zlin, Vavreckova 275, 760 01, Zlin, Czech Republic
[c] Department of Food Engineering, Suleyman Demirel University, 32260, Isparta, Turkey
[d] Department of Fat, Surfactant and Cosmetics Technology, Faculty of Technology, Tomas Bata University in Zlin, Vavreckova 275, 760 01, Zlin, Czech Republic
[e] University Institute of Technology, University of Angers, 4, Boulevard Lavoisier, BP 42018, Cedex, 19016, Angers, France
[f] Centre of Polymer Systems, Tomas Bata University in Zlin, Trida Tomase Bati 5678, 760 01, Zlin, Czech Republic
[g] CiFOOD - Center for Innovative Food Research, Aarhus University, Agro Food Park 48, 8200, Aarhus N, Denmark

ARTICLE INFO

Keywords:
Biopolymer
Essential oil
Food packaging
Food waste
Structure-properties relationship
Sustainability

ABSTRACT

Disposing food and fossil-based packaging waste is currently a huge global challenge. Bio-based active food packaging is potentially an efficient and versatile approach to reducing household and retailer waste. Active compounds released from packaging could increase food shelf-life. Compound release behavior depends on the physical and mechanical durability and strength of the active layer in contact with food. Bio-based polymers are weaker and more prone to hydrolytic degradation than fossil-fuel-derived polymers. In this study, the structure-properties relationships of mechanically and hydrolytically robust and durable bio-based zein/chitosan films with cellulose nanocrystal (CNC) filler network, containing different combinations of active compounds, were investigated pertaining to their role as a food contact layer. Different essential oils (EOs), namely thyme (TEO EO) and oregano (OEO EO), and their complex with the phenolic thymol (THY) were investigated as active compounds. EOs worked synergistically with the phenolic THY to increase the mechanical strength and durability of active film layers. The CNC-incorporated active film layers with TEO EO and OEO EO had higher mechanical strength and greater hydrolytic stability compared to non-CNC-included films, which allowed films to remain in contact with food for longer. EO addition substantially enhanced the gas barrier performance of films, and no further improvement was observed with the addition of CNC. EOs/CNC also imparted films with antimicrobial activity *in vitro*. This paper provides insights into how to design filler network-based active food packaging layers, with regards to which combination of active compounds and fillers are required for different food packaging applications.

1. Introduction

Petroleum-based fossil plastic food packaging materials and their waste are a large health, environmental, and economic concern because they are non-renewable and non-biodegradable and can leach chemicals (Zhang et al., 2022). The European Union - Packaging and Packaging Waste Regulation (PPWR) adopted a range of new measures to increase sustainability in packaging and reduce packaging waste, including introducing packaging reduction goals (5% by 2030, 10% by 2035 and 15% by 2040) (European Union, 2024). Particularly, bio-based packaging solutions can help achieve the PPWR's targets. Biopolymers obtained from renewable sources, namely polysaccharides, proteins, lipids,

* Corresponding author. Department of Environmental Protection Engineering, Faculty of Technology, Tomas Bata University in Zlin, Vavreckova 275, 760 01, Zlin, Czech Republic.
** Corresponding author. Department of Food Science, Aarhus University, Agro Food Park 48, 8200, Aarhus N, Denmark.
E-mail addresses: mjanalikova@utb.cz (M. Janalikova), iuu@food.au.dk (I. Uysal-Unalan).
[1] Authors contributed equally.

https://doi.org/10.1016/j.foodhyd.2025.111316
Received 2 October 2024; Received in revised form 20 February 2025; Accepted 2 March 2025
Available online 3 March 2025

and their blends, are seen as a viable sustainable strategy for reducing petroleum-based plastic dependency (Cruz et al., 2022; Eranda et al., 2024; Uysal-Unalan et al., 2024) by mitigating food and packaging waste.

For films or coatings, biopolymers can be directly applied to food products by casting, dipping, or spraying (Eranda et al., 2024). Alternatively, they can be deposited on thin recycled plastic packaging layers to provide safe and functional primary layers for food contact. Such layers can be tuned, and in synergy with the plastic layer, provide the necessary oxygen, light, and moisture barrier for maintaining or enhancing the shelf life of various types of food. The coating may also protect the food from the migration of unwanted contaminants from virgin or recycled plastics. Another interesting characteristic of these bio-based films and coatings is that they can be designed as active delivery systems for antimicrobials or antioxidants to further improve food product quality and acceptance (Eranda et al., 2024; Gagaoua et al., 2021; Ulloa-Saavedra et al., 2022).

One example of such biomaterials is zein, which is the prolamin fraction of corn protein. Zein is known for good film-forming properties, with higher tensile strength and lower water vapor permeability compared to other protein-based films (Jeski et al., 2022). Blending with chitosan was recently shown to improve the film properties of zein. This blended biomaterial additionally displayed potential as a natural carrier system for retaining active molecules, through hydrogen bonding and electrostatic interactions, for subsequent release to packaged foods (Li et al., 2022; Pavlátková et al., 2022; Zhang et al., 2022). Furthermore, chitosan is a waste byproduct generated from seafood processing (Santos et al., 2020) (over 10,000 tons/year of shellfish waste) (Coppola et al., 2021), and its use in food packaging reduces biowaste and increases the circularity of food production. However, such systems in the aqueous environment are susceptible to enzymatic hydrolysis (e.g. chitinase) and they are therefore rarely considered in active delivery applications due to their mechanical instability (Iñiguez-Franco et al., 2018; Sun et al., 2021; Villegas et al., 2019; Yang et al., 2016). Further investigation is therefore urgently required to assess how to design active delivery biopolymer models for humid food systems.

In this study, the effect of incorporating thyme essential oil (TEO EO) and oregano essential oil (OEO EO) with and without the phenolic thymol (THY), in zein/chitosan films was investigated. Phenolics like THY and carvacrol are primarily responsible for the antimicrobial and antioxidant activities of TEO and OEO EOs (Bassolé & Juliani, 2012; Charles et al., 2022; Giotopoulou et al., 2024; Sun et al., 2022). Thus, the phenolic THY was included to assess whether it can enhance the antimicrobial properties of films by acting synergistically with other bioactive compounds in TEO and OEO EOs. While blends of EOs with phenolics and other constituents of EOs have been reported (Bassolé & Juliani, 2012; Yakoubi et al., 2020), very few of them assessed synergistic activity in film applications (Sedlaříková et al., 2017; Sedlaříková et al., 2021). Furthermore, the release kinetics and mechanism of active molecules in response to hydrolysis and mechanical changes in films remain unclear.

Preserving or enhancing the mechanical stability of polymeric material modified with active substances is key to tailoring active molecule release in dry and humid food environments (Chen et al., 2019). Cellulose nanocrystals (CNC) were used in this study as their highly crystalline structure increases mechanical strength in food packaging (Perumal et al., 2022). CNC and biopolymers adhere to each other through H-bonding which improves the overall mechanical properties of the matrix composite. Similarly, the formation of hydrogen bonds between hydroxyl groups of CNC and biopolymers reduces available sites for interaction with water thus limiting hydrolytic degradation (Ghadermazi et al., 2019). Nanoparticles can be irreversibly adsorbed at the interfaces of oil-water, creating a densely packed layer and increasing long-term stability (Dickinson, 2017; Wardhono et al., 2019). This study aims to optimize the fabrication of zein/chitosan films enhanced with different combinations of active compounds, with or without added CNC, for food contact applications. Specifically, the physicochemical and functional properties of the films, release-kinetics of incorporated EOs, and synergistic effects of EO constituents were investigated in depth with regards to the preparation of active hydrocolloidal delivery layers that are fit for purpose for enhanced and sustainable food packaging.

2. Materials and methods

2.1. Materials

Chitosan (low-molecular-weight, ≥75% deacetylation degree), thymol (THY), and Tween 20 were purchased by Sigma-Aldrich (Prague, Czech Republic). Zein was obtained from TCI (Tokyo, Japan). CNC was purchased from the University of Maine, the Process Development Centre (Orono, Maine, USA). Two types of essential oils (*Thymus vulgaris*, TEO – Spain; *Origanum vulgare*, OEO – Romania) were supplied by Nobilis Tilia s.r.o. (Krásná Lípa, Czech Republic). Acetic acid was provided by IPL (Zlín, Czech Republic), and ethanol by PENTA s.r.o. (Prague, Czech Republic). Microorganisms were obtained from the Czech Collection of Microorganisms: Gram-negative rods *Escherichia coli* ATCC 25922, Gram-positive cocci *Staphylococcus aureus* ATCC 25923, yeasts *Candida albicans* ATCC 90028 and *Candida parapsilosis* ATCC 22019, and micromycetes *Aspergillus brasiliensis* ATCC 16404. Mueller–Hinton (MH) Agar (Himedia Laboratories, Telangana, India) was used for the growth of bacteria (37 °C/24 h). Sabouraud Agar (Himedia Laboratories, Telangana, India) was used to cultivate yeasts and molds (20 °C/5 days). Trolox (6-hydroxy-2, 5, 7, 8-tetramethylchroman-2-carboxylic acid), 2, 2-diphenyl-1-picryl-hydrazyl-hydrate (DPPH), methanol, and other chemicals were purchased from Sigma-Aldrich Co. (St Louis, MO, USA).

2.2. Preparation of films

A stock solution of chitosan (0.5% w/v) in 1.0% v/v acetic acid was prepared by dissolving chitosan in an ultrasonic bath at 40 °C for 30 min, followed by stirring until it was completely dissolved. A stock solution of zein (2.0% w/v) in 75% ethanol was prepared by dissolving a calculated amount of zein in ethanol with magnetic stirring at 500 rpm, 40 °C for 20 min, followed by ultrasonic homogenization by Hielscher UP400St (Teltow, Germany) continuously for 10 min at 50% amplitude (sonotrode type S24d3).

The concentration of active compounds (THY, TEO, OEO, or their combinations) was selected based on the previous study (Pavlátková et al., 2022) and added to the zein solution and homogenized at 500 rpm on a magnetic stirrer for 30 min at ambient temperature. Afterward, the chitosan solution (zein/chitosan, 7/1, v/v) was dropwise pipetted under continuous stirring, and then 2 mL of 5% w/v Tween 20 solution in 75% ethanol (v/v) was added with a further 30-min homogenization.

For films with CNC, CNC 0.05 or 0.1% w/v was weighed and mixed with prepared zein/chitosan/EO or zein/chitosan/EO/THY solution by stirring at 500 rpm on a magnetic stirrer for 30 min and ultrasonicated for 10 min at 50% amplitude. Analogously, as a control, a sample without active substance and CNC was prepared. The prepared biopolymer film solutions (25 mL) were poured into plastic Petri dishes (9 cm diameter) in a laminar box and then dried in an oven at 35 °C for 24 h. The dried films were kept at room temperature at ~ 60% RH. The thickness of films was measured with a digital micrometer (Schut, Trossingen, Germany) at an accuracy of 0.001 mm, and the average of ten measurements was reported as 100 μm for control, 108–115 μm from EOs and EOs/THY films and 121–128 μm for EOs/CNC and EOs/THY/CNC.

The composition and designation of films are summarized in Table 1.

2.3. Zeta potential and pH measurement of film-forming solutions

The zeta potential measurements of polymer solutions were carried

Table 1
Designation of hydrocolloidal polymeric film systems.

Films	Thyme EO (w/w, %)	Oregano EO (w/w, %)	Thymol (w/w, %)	CNC (w/v, %)
[a]Control	–	–	–	–
TEO	2	–	–	–
TEO/CNC 0.05	2	–	–	0.05
TEO/CNC 0.1	2	–	–	0.1
OEO	–	2	–	–
OEO/CNC 0.05	–	2	–	0.05
OEO/CNC 0.1	–	2	–	0.1
TEO/THY	2	–	2	–
TEO/THY/CNC 0.05	2	–	2	0.05
TEO/THY/CNC 0.1	2	–	2	0.1
OEO/THY	–	2	2	–
OEO/THY/CNC 0.05	–	2	2	0.05
OEO/THY/CNC 0.1	–	2	2	0.1

[a] Control = base film: zein + chitosan; used as the basis for the remaining films.

out at 25 ± 1 °C in triplicate using a Zetasizer model Nano ZS device Malvern Instruments, Ltd. (Malvern, UK) after diluting the samples with 75% (v/v) ethanol.

The pH of solutions was measured in triplicate using a pH meter Metrohm 913 and a spearhead electrode Metrohm (Metrohm AG, Herisau, Switzerland) at room temperature.

2.4. Scanning electron microscopy

Morphology of the surfaces and cross-sections of films was visualized using a scanning electron microscope (SEM) Nova NanoSEM 450 with Schottky field emission electron source operated at an acceleration voltage of 30 kV (Thermo Fisher Scientific, Brno, Czech Republic). The films for SEM analysis were prepared by crushing, following freezing in liquid nitrogen. The prepared samples were coated with a 10 nm thick Au/Pd layer by magnetron sputtering before the inspection.

2.5. Fourier transform infrared spectroscopy

Fourier Transform Infrared Spectroscopy (FTIR) spectra were recorded on an Alpha-T FTIR spectrometer (Bruker, Billerica, MA, USA). The spectrum was recorded in the spectral range from 400 to 4000 cm^{-1} with a resolution of 4 cm^{-1} (32 scans). All the FT-IR spectra were baseline-corrected and evaluated using the OPUS program (version 7.5).

2.6. Moisture content and hydrolytic degradation behavior of films

Moisture content was measured thermo-gravimetrically at 105 °C by using a moisture analyzer (Mettler Toledo, HR73 Halogen Ohio, USA) that operates with a halogen dryer unit. The results were calculated as an average of three replicates.

The hydrolytic degradation behavior of films was performed under the buffered condition using phosphate salt saline buffer (PBS, pH 7.4) in water at 23 °C. Films were cut into 2 × 2 cm sizes and dried before degradation analysis. Films were then stored in sealed glass vials containing 25 mL of PBS for 168 h pH of the degradation medium was also recorded when the hydrolysis test started and was completed. During the test, the changes in the film structure were tracked visually at predetermined time intervals. At the end of the test, the obtained solutions containing remaining film piece(s) were filtered on a glass microfiber filter (Whatman™; diameter 25 mm; pore size 20 μm) and dried at room temperature until no weight changes were observed and measured gravimetrically.

2.7. Determination of release profiles

Samples of the size 3 × 3 cm were cut from the dried films, weighed at the accuracy of 0.0001g, inserted into glass bottles with 30 ml PBS buffer (pH 7.4), achieving an area-to-volume ratio of 3 dm^2/L, and incubated at 4 and 23 °C with constant agitation at 50 rpm. At defined intervals up to 48 h, three 2 ml aliquots of release medium were taken and replaced with fresh buffer. The samples were then analyzed by UV visible spectrophotometer (VWR UV-3100PC, USA) at the wavelength of 273 nm where maximum absorption for THY and carvacrol, the main constitutes of TEO and OEO EOs, were previously reported (Charles et al., 2022; Giotopoulou et al., 2024; Sun et al., 2022). The release curves were obtained by plotting the measured contents (mg/cm^2) over time (h), and the slope of the initial linear portion of these formed curves was used to determine the initial release rates (mg/cm^2/h) of relative film samples. Peleg's equation (Peleg, 1988) was also used to model the release kinetics using Equation (2):

$$M_t = t / [(k_1) + (k_2 t)] \quad (1)$$

where M_t is the amount of active compound released at each time, and the kinetic constants, k_1, and k_2, are the inverse of the initial release rate and the inverse of the asymptotic release value, respectively.

The total soluble phenolic content released from film samples into the PBS medium was also determined spectrophotometrically at both 4 and 23 °C for 48 h (Singleton & Rossi, 1965). Briefly, the taken release medium was treated with Folin–Ciocalteu reagent (0.2 N) and sodium bicarbonate (7.5%, w/w) before reading absorbance at 765 nm (Synergy, BioTek multimode microplate reader with Gen5 software, Bio-Tek Instruments, Inc.). The results were expressed as gallic acid equivalent (GAE) per cm^2 of film samples using the gallic acid calibration curves.

The discoloration of dark, purple-colored DPPH free radicals by the released active compounds from film samples at 4 and 23 °C was also monitored until the active compound release reached equilibrium. Briefly, an aliquot of release medium was subjected to DPPH radical, and the mixture was incubated at 23 °C for 40 min before reading absorbance at 517 nm (Synergy, BioTek multimode microplate reader with Gen5 software, Bio-Tek Instruments, Inc.). The results were expressed as mg Trolox/cm^2 of film sample using the Trolox (40–160 μg/mL) calibration curves, and DPPH inhibition percentages calculated from the loss of absorbance by dividing the reduction in absorbance by the absorbance of DPPH solution.

2.8. Antimicrobial activity of films

The antimicrobial activity of the prepared films was determined by the disk diffusion method against *S. aureus, E. coli, C. albicans, C. parapsilosis,* and *A. brasiliensis*. Disks with a diameter of 9 mm were cut from the prepared films. The prepared agar media (MH, Sabouraud) were poured into Petri dishes and solidified. 1 ml of the stock inoculum (bacteria, yeasts, or fungi) was evenly spread onto the solidified agar media agar where film discs were later placed. Petri dishes were incubated according to the microorganisms in place (bacteria at 37 °C/24 h; yeasts and fungi at 25 °C/5 days). After incubation, the diameters of the inhibition zones, including the area under the disk, were measured. The experiments were performed in triplicate.

2.9. Statistical analysis

All experiments were performed at least three times, and the data were expressed as mean ± standard deviation. The statistical analyses were performed using Minitab® 17 with Tukey's multiple comparison tests at a two-sided 95% confidence level. The obtained data were analyzed to evaluate the differences between the films with one-way

ANOVA. Release kinetics data were also analyzed to assess the significance of the film type and release medium temperature, and their interactions, using two-way ANOVA. Besides, the Pearson correlation coefficient was used to assess the relationship between phenolic content and DPPH radical scavenging activity of films, with statistical significance determined at $\alpha = 0.05$.

3. Results and discussion

3.1. Zeta potential and pH of film-forming solutions

Zeta potential is related to the net surface charge of the liquid system resulting from the interaction between particles and biomolecules. It is a crucial factor for determining the colloidal stability of charged particles associated with adsorption, aggregation, and dispersion mechanisms, and understanding the performance of the system under a variety of conditions. A higher tendency to aggregate causes the stability to drop dramatically when the zeta potential value is in the range 0 to ±10 mV. On the other hand, systems possessing a sufficiently positive (>+30 mV) or negative (<−30 mV) zeta potential value are more stable (Gurpreet & Singh, 2018).

As reported in Fig. 1, the zeta potential values of prepared zein/chitosan film-forming solutions with EOs and EOs/CNC exceeded the +30 mV threshold, indicating sufficient electrostatic stability, except for the film containing TEO EO.

This is because, contrary to OEO EO, TEO EO has a larger number of negatively charged ions in its functional groups (González-Reza et al., 2021). This might have caused zein particles to inhomogeneously adsorb to the surface of TEO droplets through hydrogen bonding and mechanical interlocking, causing the diffusion of some of TEO to the surface and reducing net surface charge (∼ +20 mV) compared to the control film (∼+33 mV). On the other hand, the addition of THY together with the TEO EO substantially increased the zeta potential of the film-forming solution (TEO/THY) compared to the TEO film-forming solution. This behavior can be explained by the fact that TEO with THY formed a strong complex such that the surface successfully interacted with zein/chitosan through electrostatic and hydrophobic interactions. Likewise, CNC contains numerous hydroxyl groups and electronegative atoms (Zhang et al., 2021) that can form hydrogen bonds with positively charged chitosan, thus the incorporation of CNC increased film stability indicated by higher zeta potential values in the corresponding films.

The pH values of all prepared film-forming zein/chitosan solutions were found between 5.5 and 5.6, which are similar to results obtained by Pavlátková et al. (2022) for zein/chitosan active film-forming solutions.

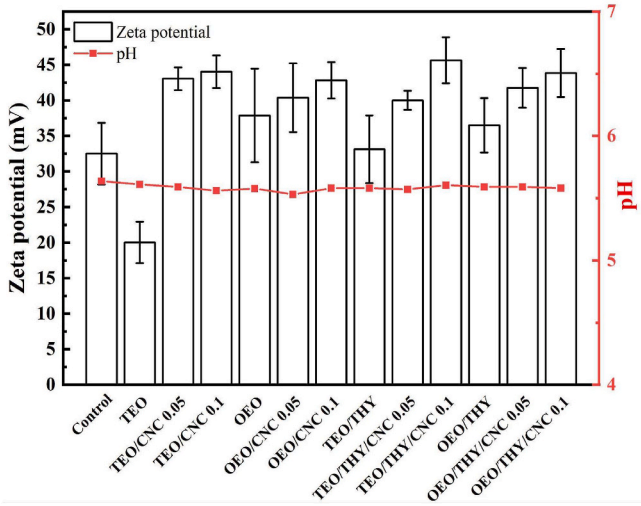

Fig. 1. Zeta potential and pH values of hydrocolloidal polymeric film solutions.

Reported values were below the isoelectric points of chitosan (pI = 6.2) and zein (pI = 6.5).

3.2. Changes in microstructure and specific surface area

Microstructural changes in films were observed following the incorporation of bioactive compounds and CNC by SEM micrographs in Fig. 2.

The control film without active molecules or CNC had a coarse structure with irregularly shaped folds and particles, formed probably due to the entanglement of polymer chains in the zein/chitosan mixture (Zhang et al., 2019). On the other hand, the structure of TEO films was relatively homogenous with uniformly distributed droplets due to the TEO EO. In the case of OEO EO, the film surface was still relatively rough; furthermore, the cross-section of the film appeared bumpy with randomly occurring pores. Films containing TEO or OEO EOs in combination with THY become smoother on the surface without any apparent cracks or pores, indicating good compatibility between the two compounds, which agrees with the outcome of work by Sedlaříková et al., 2019. Larger droplets seen on the surface of TEO films (Fig. 2), based on the study of Souza et al. (2021), might have been caused by insufficient energy to break the larger droplets while still preserving solution stability, which is not aligned with the lower zeta potential of TEO films reported in this study (Fig. 1). It is possible that the presence of larger droplets was instead formed due to flocculation which might have reduced solution stability, as indicated by a zeta potential.

Adding CNC also affected the film microstructure (Fig. 2). In the case of TEO/CNC films, the difference was most evident on the surface, where a high concentration of tiny droplets was observed. On the other hand, the surface of TEO/THY/CNC, OEO/CNC and OEO/THY/CNC films were relatively smooth, while their cross sections were highly porous. The porous structure observed within the microstructure of films with CNC could be due to the generation of microbubbles by the ultrasonic sound waves during the process by which CNC was added to film-forming solutions and mixed by highly intensive ultrasonication. Similar results were reported by Alves et al., 2015, who found the air microbubbles on the cross sections of starch films containing CNC as a result of the film preparation process at the high speed of mixing.

3.3. Molecular interactions in the colloidal film systems and the associated mechanisms

Molecular interactions in films were investigated by the Fourier transform infrared spectroscopy (FTIR) spectroscopy (Fig. 3).

The spectrum of the control film shows characteristic peaks of zein and chitosan polymers at 3290–3280 cm^{-1} (the stretching of N-H and hydrogen bonding), 2925–2960 (C–H stretching), 1650–1646 cm^{-1} (the stretching of C=O, amide I), 1547–1558 cm^{-1} (the stretching of C–N, amide II), 1410–1420 cm^{-1} (the stretching of -C–N), 1230–1250 cm^{-1} (the stretching of C–N and the bending of N–H, amide III). Also, the peak around 1000–1050 cm^{-1} was associated with −OH deformation (Deng et al., 2018; Zhang et al., 2019). Incorporating individual EOs and EOs/THY complexes into films gave rise to new peaks at 806 cm^{-1} and 860 cm^{-1}, due to aromatic ring vibrations of THYs (Schulz et al., 2003). This indicates that EOs and their complex were effectively loaded in the colloidal polymer systems. The peak intensities in the different regions of the spectra were suppressed when CNC was added to films along with the TEO or EOs. This behavior can be explained by the preferential binding of the zein/chitosan blend to CNC compared to TEO or OEO EOs as a consequence of higher-intensity hydrogen bonding and/or electrostatic interactions (Xue et al., 2021), which hinders the interaction between the EOs and the polymer blend. However, the reduction pattern in peak intensity, when CNC was added, was not observed for the films with TEO/THY or OEO/THY complexes, revealing that most of the binding sites of polymer blends were already occupied by the TEO/THY or OEO/THY complexes before CNC was incorporated.

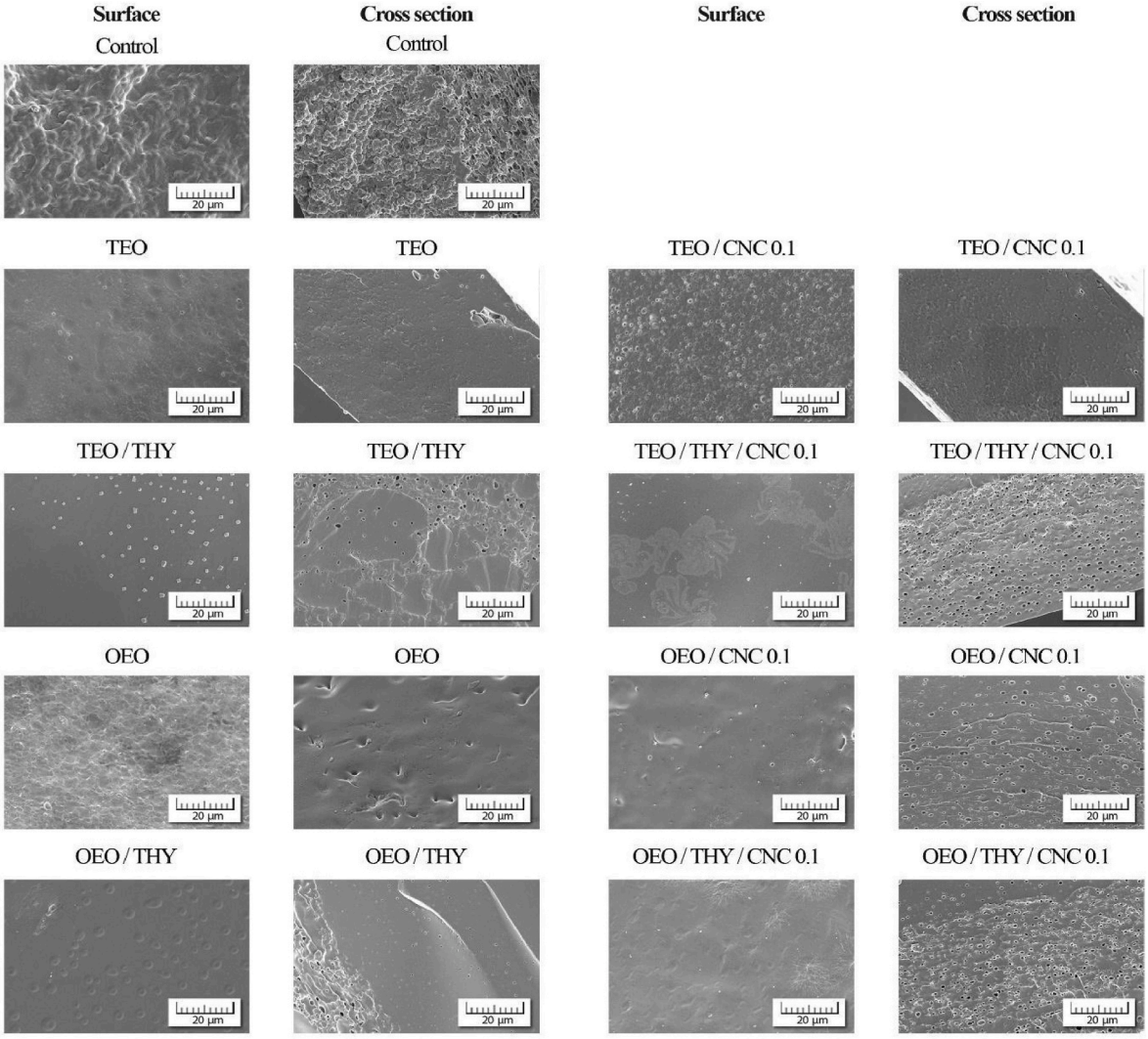

Fig. 2. SEM images of surfaces and cross-sections of hydrocolloidal polymeric film systems.

The inclusion of all EO combinations either shifted FTIR peaks slightly or introduced new peaks altogether in the 800-1100 cm^{-1} range relative to the control film. Including CNC, it led to the broadening and shifting of FTIR peaks in TEO and OEO films, while no change was observed in the FTIR spectra of TEO/THY and OEO/THY films. This observation further suggests that the addition of CNC to TEO and OEO promotes interactions unlike CNC and TEO/THY or OEO/THY.

A possible mechanism of interactions between each component in hydrocolloidal film systems is depicted in Fig. 4.

Zein is a protein composed of prolamine proteins, including alpha-zein, beta-zein, gamma-zein, and delta-zein, which contribute to its hydrophobic nature (Luo and Wang, 2014). The hydrophobic nature of zein allows it to interact with hydrophobic compounds such as THY and carvacrol through hydrophobic interactions, van der Waals forces, and potentially hydrogen bonding (Luo and Wang, 2014). Chitosan, on the other hand, is a cationic polymer due to the presence of amino groups, which allows it to interact with negatively charged molecules or surfaces through electrostatic interactions, such as hydrogen bonding and ionic interactions (Aranaz et al., 2021). The hydrophobic nature of zein can interact with the cationic nature of chitosan, resulting in improved film properties, stability, and controlled release of encapsulated compounds (Zhang et al., 2022). THY, similar to carvacrol, consists of a phenolic ring with a hydroxyl group (-OH) and a methyl group (-CH_3) (Ramos et al., 2013). Therefore, zein or chitosan can immobilize active compounds such as THY or carvacrol present in TEO and OEO EOs through various techniques such as electrostatic complexation, coacervation, or emulsification (Granata et al., 2021), which become a tool to adjust the desired release behavior. These interactions are further suggested by the new peaks occurring at 806 cm-1 and 860 cm^{-1} in FTIR spectra (Fig. 3). Furthermore, the possible van der Waals interactions or hydrogen bonds between THY and the active compounds of EOs when combined with THY, are associated with those new peaks observed at approximately 1200 and 800 cm^{-1}. Additional interactions, such as hydrogen bonding or electrostatic interactions, can further stabilize the encapsulated compounds. The molecular structure of CNCs consists of parallel, tightly packed cellulose chains arranged in a crystalline lattice where each cellulose chain is composed of repeating glucose units joined together by β-(1 → 4) glycosidic linkages (Nguyen et al., 2019). The glucose units are in the form of D-glucose, and the primary hydroxyl groups (-OH) on the cellulose chains are oriented towards the surface of the nanocrystal. Thus, the interactions between zein/chitosan and CNC can involve hydrogen bonding, electrostatic interactions, and entanglement of polymer chains, leading to enhanced film properties (Mortier et al., 2022; Pires et al., 2021) that was proven with the shift in the peaks of 900–1200 cm^{-1} range.

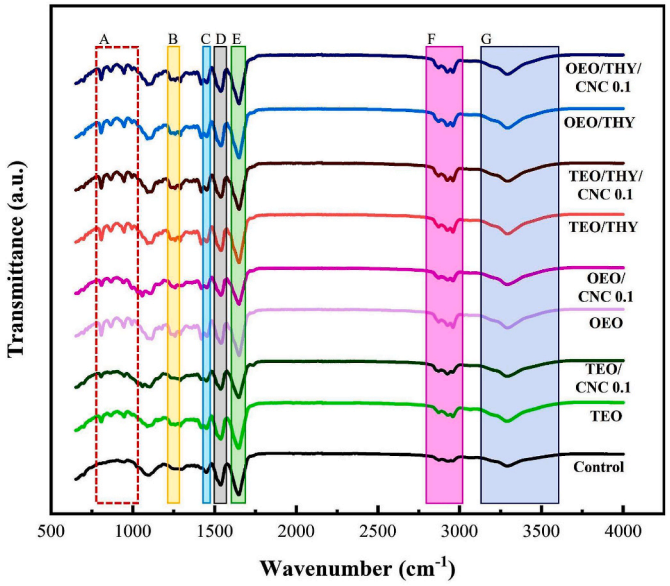

Fig. 3. FTIR spectra of hydrocolloidal polymeric film systems (A = new peaks; B = C-N stretching, N-H bending, amide III; C = -C-N stretching; D = C-N stretching, amide II; E = C=O stretching, amide I; F = C-H stretching, G = OH bonding, N-H stretching).

3.4. Thermal, barrier, and mechanical properties of films

Bio-based films and coatings are commonly produced by solvent casting due to their incompatibility with melt processing. They are thus applied as a food contact layer on primary plastic or paper packaging (Asgher et al., 2020; Kunam et al., 2022). However, they are gaining more momentum as primary plastic coatings or as edible films and coatings wrapped onto food surfaces that can be later heat-treated by microwave heating (Reichert et al., 2020; Tyagi et al., 2021). At the end of their use, depending on implementation, they can be composted together with carryover food waste, or sent for recycling together with primary plastic/paper packaging (a package containing up to a 5% layer by weight of other materials is considered compatible with postconsumer plastic/paper recycling stream), or incinerated, which is not considered as sustainable waste treatment (Sampaio et al., 2023; Schmidt et al., 2022). Understanding the thermal stability of packaging films and coatings could inform application, use, and after-use strategies. In this study, the thermal behavior of films was studied by TGA from 25 to 600 °C (Fig. S2 and Table S2). The first weight loss occurred around 70–110 °C due to the evaporation of water while the second phase was between 180 and 200 °C, which might be related to devolatilization, active pyrolysis stage, or partial decomposition of EOs as reported in Fig. S1 and Table S1. The major weight loss occurred in the third phase, due to the decomposition of the primary protein backbone of the zein and chitosan complex (Mendes et al., 2020; Wang et al., 2017). The main decomposition temperature for the control film was ~331 °C while the addition of EOs (TEO or OEO) individually or as a complex with a THY increased decomposition temperatures slightly to ~ 332–333 °C. However, the CNC inclusion in the film matrix reduced decomposition temperature by 1–2° (~330–331 °C). No significant difference in the thermal stability of films was observed from adding EOs and/or CNC (Table S2). Similarly, Li et al. (2022) and Xue et al. (2021) observed a slight increase in decomposition temperatures of films to ~ 332–333 °C following EO addition, which could be due to

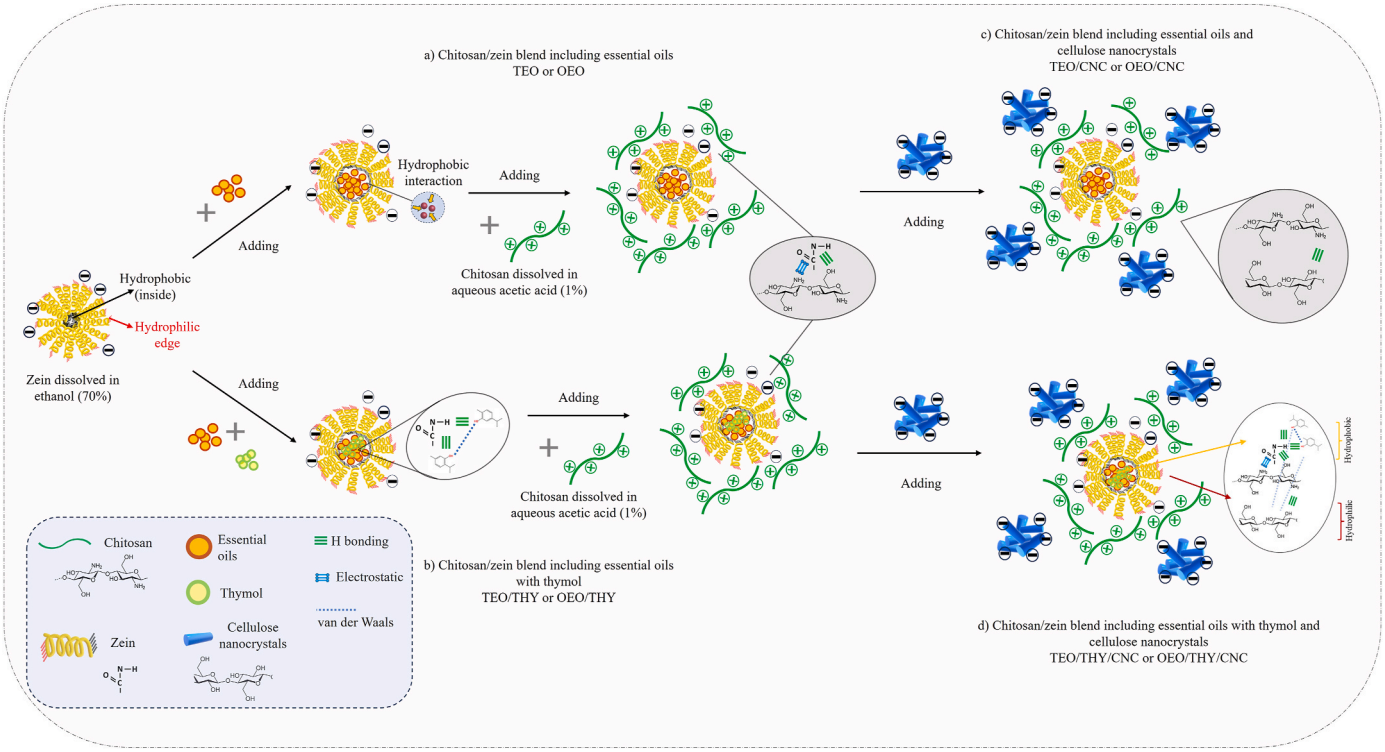

Fig. 4. The possible mechanisms of interactions occurring between components (a) Interaction between zein and chitosan includes hydrogen bonding through NH and OH groups and electrostatic interactions through negative charges of zein and positive charges of chitosan, whereas including hydrophobic interaction between EOs and zein occur through the hydrophobic residues of zein, (b) in addition to the interactions explained at (a) including interactions between THY and TEO EO or THY and OEO EO through the hydrogen bonding between OH groups of oils and/or van der Waals interactions between oils, (c) in addition to the interactions explained at (a) including interactions between cellulose nanocrystals and chitosan through the hydrogen bonding between NH_2 groups of chitosan and OH groups of cellulose, (d) in addition to the interactions explained at (b) and (c) including interactions between functional groups of each component via hydrogen bonding, electrostatic and van der Waals interaction.

intermolecular changes.

Another important feature to consider in choosing packaging materials is the gas and water vapor barrier performance, which is critical in maintaining food quality during shelf life (Chen et al., 2022). It is worth noting that the optimal OP and WVP values may vary depending on the intended use of the packaging material and packaging technology such as vacuum skin packaging or modified atmosphere packaging. The permeability values of all films are reported in Table S2. Generally, most biopolymers underperform in oxygen and water vapor barrier compared with conventional polymers, which limits their use as a primary monolayer packaging. For example, the WVP of chitosan films is known to be approximately one order of magnitude higher than that of low-density polyethylene (LDPE) (Cazón et al., 2022). In this study, blending chitosan with zein together and EOs was found to be a successful and sustainable strategy for enhancing the water vapor barrier, while CNC addition in almost all cases did not increase the barrier performance in the films. This phenomenon may be due to the low cohesion and high porosity of the films, which did not reduce the penetration of WP through the continuous layer (Liu, Song, Chen, Deng, Chao, Yang, Wu, Bai, Zhang & Hu, 2022). While some studies indicated that CNC-added films had higher barrier properties compared to control films, this positive effect was concentration-dependent and only observed when CNC was added at high concentrations, e.g. 1–6%, (Hamedi et al., 2024; Salari et al., 2018). This is at least 10-fold higher compared to our film systems. The addition of EOs to films decreased OP significantly and while combining EOs with CNC increased this slightly, the OP values were still lower than for the control film. This indicates potential use as oxygen-barrier layers. The critical message from these findings is that the intended food application of the packaging material should be considered when selecting the required barrier material.

When it comes to the mechanical performance of packaging films (Table S2), the control film was too brittle and unable to resist applied tensile loads. Thus, it could not be evaluated for its tensile properties. A major obstacle in using zein/chitosan films was overcome, on the other hand, by adding EOs. Films that included EOs or EOs/THY exhibited higher elasticity (6–49%) and were accordingly more resistant to fracture during stretching. The maximum extension was recorded following the addition of OEO EO and THY; however, CNC incorporation reduced film elongation ($p < 0.05$), possibly due to higher crystallinity and relatively restricted polymer chain mobility, which is consistent with other works (Fernandes et al., 2009; Soofi et al., 2021). However, overall CNC increased film strength, due to the strong interfacial adhesion between CNC and the chitosan matrix resulting from hydrogen bond and electrostatic interaction between the cationic groups of chitosan and anionic sulfate groups of CNC (Chi & Catchmark, 2018).

3.5. Moisture content and hydrolytic stability of films

The moisture content of the control film was 4.9% ± 0.6. Adding EOs reduced the moisture content values of films to 3.2–4.2%. EO mainly contributes to covalent bond formation between the functional groups of chitosan chains, lowering availability of its hydroxyl groups thus limiting polysaccharide-water interactions (de Oliveira Filho et al., 2020).

Although many studies on active food packaging systems have been reported, only a few of them have investigated hydrolytic stability and its evolution during its use as part of polymer systems' development and testing. Nonetheless, this is crucial for their intended applications (Chen et al., 2024; Iñiguez-Franco et al., 2018). In the view of food packaging applications, in particular, for active delivery systems, investigating and understanding the hydrolytic stability and durability of active films is needed to ensure that release mechanisms remain unaffected by film degradation. This may improve the design of active packaging films and coatings with regards to maintaining hydrolytic stability and desired release mechanism under relevant conditions throughout the shelf life to maintain food quality and safety. In this study, hydrolytic degradation of films was investigated under aqueous conditions with PBS at pH 7.4 during 168 h using gravimetric (weight loss) and visual inspection techniques (Fig. 5).

As a common approach, blending cellulose with natural and synthetic polymers increases the hydrolytic stability of chitosan in aqueous suspensions. However, such complexes are destabilized by pH or salt concentration changes. This instability limits their application in active packaging (Gupta et al., 2001). Protonation of hydroxyl and amine groups under acidic conditions makes the chitosan films water-soluble (Wang et al., 2017). On the other hand, zein is more hydrophobic due to its nonpolar amino acid content and low concentration of charged amino acids (Shukla & Cheryan, 2001). As seen in Fig. 5, following the inclusion of EOs, the zein/chitosan film changed from yellow to whitish-yellow due to the increased crystallinity induced by hydrolysis (Vahedikia et al., 2019). This indicates rapid water uptake by the films in the first 6h of hydrolytic degradation. The color transition was most evident in the zein/chitosan control films, with a corresponding mass loss of >80% in the 96 h of the test period. While the zein/chitosan control film was destroyed during the degradation test (168 h), mass loss was reduced to 20.7–70.0% by the inclusion of EOs (Fig. 5). On the other hand, the color of EO/CNC films was slightly affected by contact with PBS media during the first 6 h and remained unchanged until the completion of the degradation test. In addition, combining EO with CNC improved structural integrity substantially, as indicated with just 19.7–36.0% mass loss. In particular, the remaining mass of TEO/CNC and OEO/CNC films after the degradation was twice that of TEO and OEO films. Such enhancement in the hydrolytic stability compared to control and EO-added films confirms CNC's potential as a hydrolytic stabilizer. This could arise from the increase in zein/chitosan network formation with adequately dispersed components, thus avoiding the interruptions by hydrolytic groups (hydroxyl or amine) of chitosan (Yuan et al., 2016). From a similar perspective, including CNC might have promoted the EOs to interact with the esters and amino acid groups of zein (Vahedikia et al., 2019). Giteru et al. (2019) stated that the adequate dispersion and increased hydrophobicity made zein/chitosan-based films less soluble in aqueous systems. In addition, film degradation was also evaluated in terms of pH changes at the end of degradation (Table 2). The chemical compounds released by the polymeric hydrocolloid films during their degradation can come from the polymer itself or can be additives that are added to the polymer. Some of these degradation product compounds can reduce pH. A high degree of degradation in the control film increased the release of degradation products into the buffer and reduced pH from 7.4 to 7.07. In fact, films with the complex of EOs with THY or CNC resulted in higher pH values (7.27–7.33) in the medium compared to the other films, indicating a lower degree of degradation. This was in agreement with microstructure surface images of films OEO/CNC, OEO/THY, and TEO/THY showing a more compact and smoother surface in contrast to control and only EO-added films (Fig. 2). As an exceptional case, only TEO/CNC films developed rougher surface-based SEM images by the addition of CNC, resulting in less structural stability over the degradation period (Fig. 5).

Hydrolytic degradation of polymers takes place either from bulk erosion or surface erosion (Iñiguez-Franco et al., 2018, 2018b; Sun et al., 2021). Very few studies, however, have so far addressed its importance in active delivery applications (Sun et al., 2021; Villegas et al., 2019; Yang et al., 2016). Surface erosion mainly occurs in the near-surface region. During surface erosion, the film can become thinner, transparent, or even broken after degradation, while the initial shape is maintained. Controlled delivery systems have favored surface erosion over bulk erosion as diffusion is considered to occur instantaneously (Iñiguez-Franco et al., 2018; Vieira et al., 2013) and because the release and degradation rates are correlated. Visual inspection analysis (Fig. 5 and Fig. S3) revealed a more porous sample microstructure (Fig. 2), suggesting surface erosion rather than a bulk degradation mechanism. The addition of CNC and EOs might have increased zein/chitosan network formation, thus avoiding the interruptions by hydrolytic groups

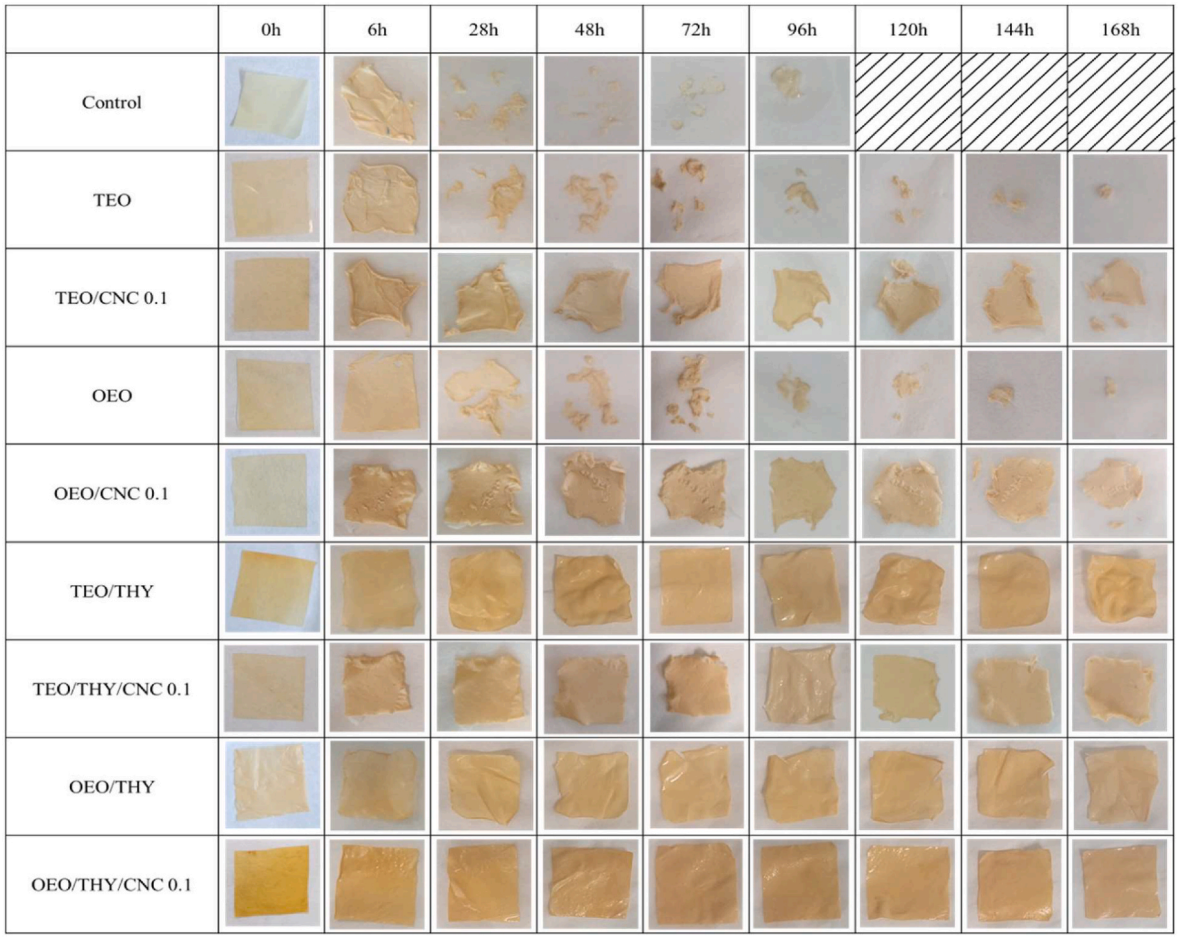

Fig. 5. Visual inspection of hydrocolloidal polymeric film systems during hydrolytic degradation.

Table 2
Moisture content, pH values, and weight loss at the end of hydrolytic degradation of hydrocolloidal polymeric film systems.

Films	Moisture content (%)	pH	Weight loss (%) at the end of hydrolytic degradation
Control	4.9 ± 0.6^{a}	7.07 ± 0.03^{d}	-[a]
TEO	4.2 ± 0.7^{a}	7.20 ± 0.01^{c}	70.0 ± 0.2^{a}
TEO/CNC 0.1	4.2 ± 0.5^{a}	7.28 ± 0.05^{ab}	36.0 ± 0.7^{b}
OEO	3.2 ± 0.5^{a}	7.21 ± 0.01^{c}	69.8 ± 1.3^{a}
OEO/CNC 0.1	4.6 ± 0.7^{a}	7.27 ± 0.07^{b}	32.0 ± 2.1^{b}
TEO/THY	3.2 ± 0.1^{a}	7.27 ± 0.03^{b}	24.6 ± 1.7^{bc}
TEO/THY/CNC 0.1	4.5 ± 0.5^{a}	7.35 ± 0.05^{a}	23.8 ± 1.4^{bc}
OEO/THY	4.0 ± 0.6^{a}	7.29 ± 0.04^{ab}	20.7 ± 1.6^{cd}
OEO/THY/CNC 0.1	4.1 ± 0.8^{a}	7.33 ± 0.03^{a}	19.7 ± 1.2^{d}

Different letters in the same column are significantly different based on Tukey's test ($p < 0.05$).
Results mean ± standard deviation ($n = 3$, at least).
[a] It was not possible to collect the film samples from the aqueous medium as the remaining was very little and like a tiny powder.

(hydroxyl or amine) of chitosan. This type of improvement could be associated with the changes in the FTIR spectra, seen as the intensity of the peaks and the appearance of new peaks, supporting better interactions between the components of the films and their stability during hydrolytic degradation (Mathew et al., 2006).

3.6. Release behavior of essential oils from films and the associated mechanism

In antimicrobial and antioxidant active food packaging, understanding the release behavior mechanism of bioactive substances from the polymer matrix is essential to effectively enable the designing of tailor-made release systems for targeted food and food model systems. Such systems can result in significant benefits, including food waste reduction, conversion of by-products e.g. chitosan to value-added materials, and reduced dependency on fossil-based plastic.

Evaluating the release of active compounds into food is even more challenging due to the complexity of food matrices where nutrients and non-nutrients interact physically and chemically (Crowe, 2013; Manzanarez-López et al., 2011). Primary physical factors that affect the release kinetics are the nature of the polymer, and solubility (Fernández-Pan et al., 2015). In this work, the release from packaging systems was studied, in which the release behavior of individual and combined active EOs and their effect in combination with CNC from zein/chitosan polymer matrix into PBS medium was evaluated. The release profiles, total released phenolic content, DPPH scavenging activity of films, and the relationship between total released phenolic content and DPPH scavenging activity at 4 and 23 °C are shown in Figs. 6–9. Release curves were also subjected to model fitting, and the overall fitting of experimental data was good for each sample (Fig. 6).

Table 3 reveals the relative release kinetics of films. The EO release rates were greatest in TEO and OEO films at 4 and 23 °C, which were 2–2.5 times higher than those for TEO/THY and OEO/THY films respectively. This could be due to increased water resistance when combining two EOs. Unalan et al. (2013) also suggested that the

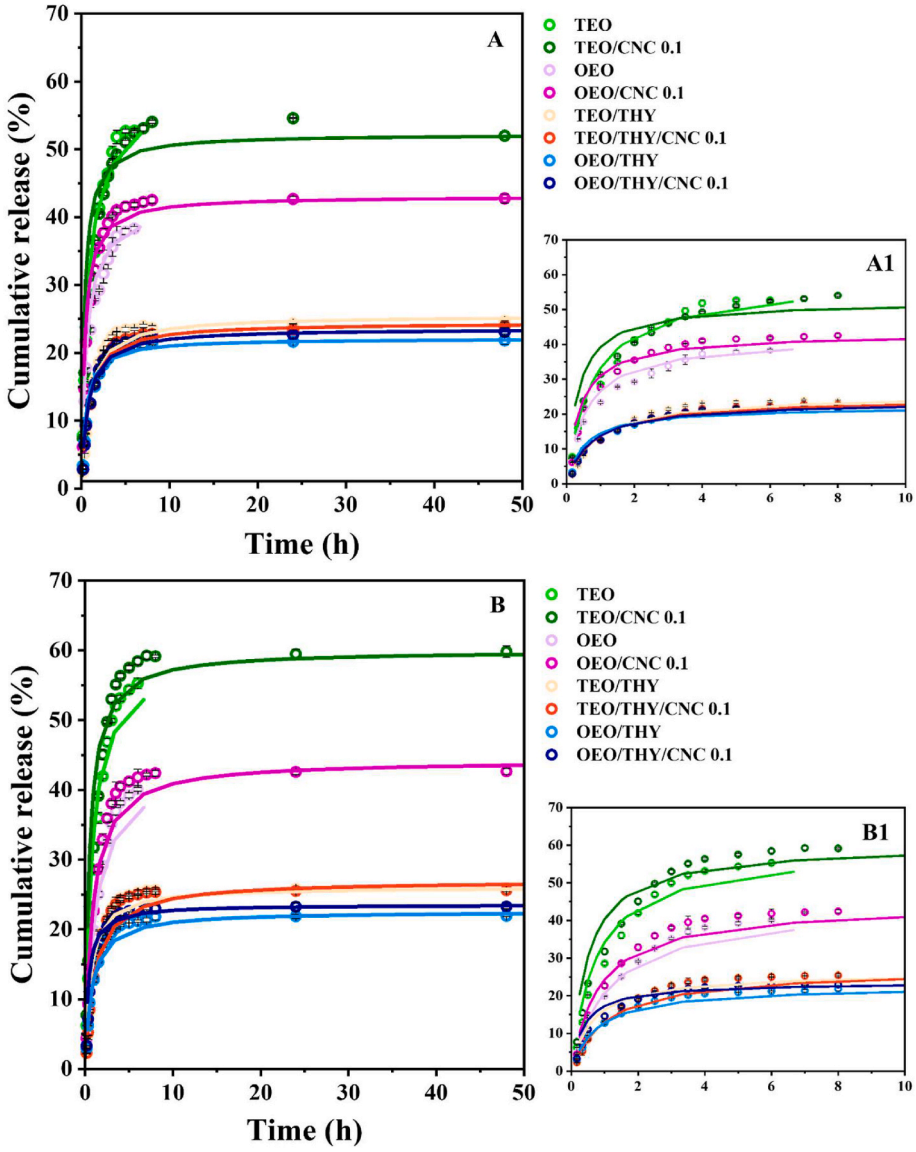

Fig. 6. Release profiles of hydrocolloidal polymeric film systems at 4 (A) and 23 °C (B) (experimental data points with Peleg fitted model with lines). Figures A1 and B1 are the zoom portions of figures A and B, respectively, during the first 10 h.

reduction in release rates of lysozyme in zein films with and without gallic acid and catechin was due to increased hydrophobicity and tortuosity of films resulting from wax addition.

As shown in Fig. 6, the release behavior of the films at 4 and 23 °C were similar and the addition of CNC slightly increased the initial release rates of films. All films displayed a very fast release within 1–2 h and gradually decreased in release rate reaching the equilibrium between 8 and 24 h at 4 °C and 23 °C. Similarly, Chen et al. (2020) observed a fast release within 120–150 min, which gradually slowed down the release of tea polyphenols and OEO EO from zein/gelatin composite films. However, Kashiri et al. (2017) reported a faster release followed by a slower release reaching equilibrium within 1 h at 37 °C and 18 h at 4 °C for the release of carvacrol and THY from zein-based films.

The highest cumulative release content was observed in TEO and TEO/CNC 0.1 films (about 55%) followed by OEO and OEO/CNC 0.1 films (about 40%) and the films including the combination of EOs with or without CNC presented the lowest release content (about 20–25%) at storage temperatures. Even though, due to its hydrophilic character, the loading of CNC increased the rate of release of active compounds in the early stage slightly compared to their CNC-free counterparts, the combination of EOs played a significant role in controlling the rate of release and diffusion path with the combination of polymer swelling behavior (Deng et al., 2019). Similar results were also reported by Lee et al. (2018) and Lian et al. (2019) for the release of clover EO from chitosan films in the presence of halloysite nanotubes and the release of TEO EO from chitosan films in the presence of hydrophilic-lipophilic balance emulsifying agents, respectively.

The phenolic activity of EOs released into the medium was also screened by measuring the total phenolic amount and antioxidant activity by Folin Ciocalteu and DPPH radical scavenging activity tests, respectively, during the release test until reaching the equilibrium (Table 4). The total phenolic content (based on the gallic acid equivalent) and the antioxidant activity (based on the Trolox equivalent) of films were varied by the type and number of active compounds. Importantly, the addition of CNC positively influenced the mechanical integrity of films when they came in contact with water/buffer, resulting in longer activity which is critical for active delivery systems (Figs. 7 and 8).

TEO/THY/CNC 0.1 film showed the highest total phenolic content

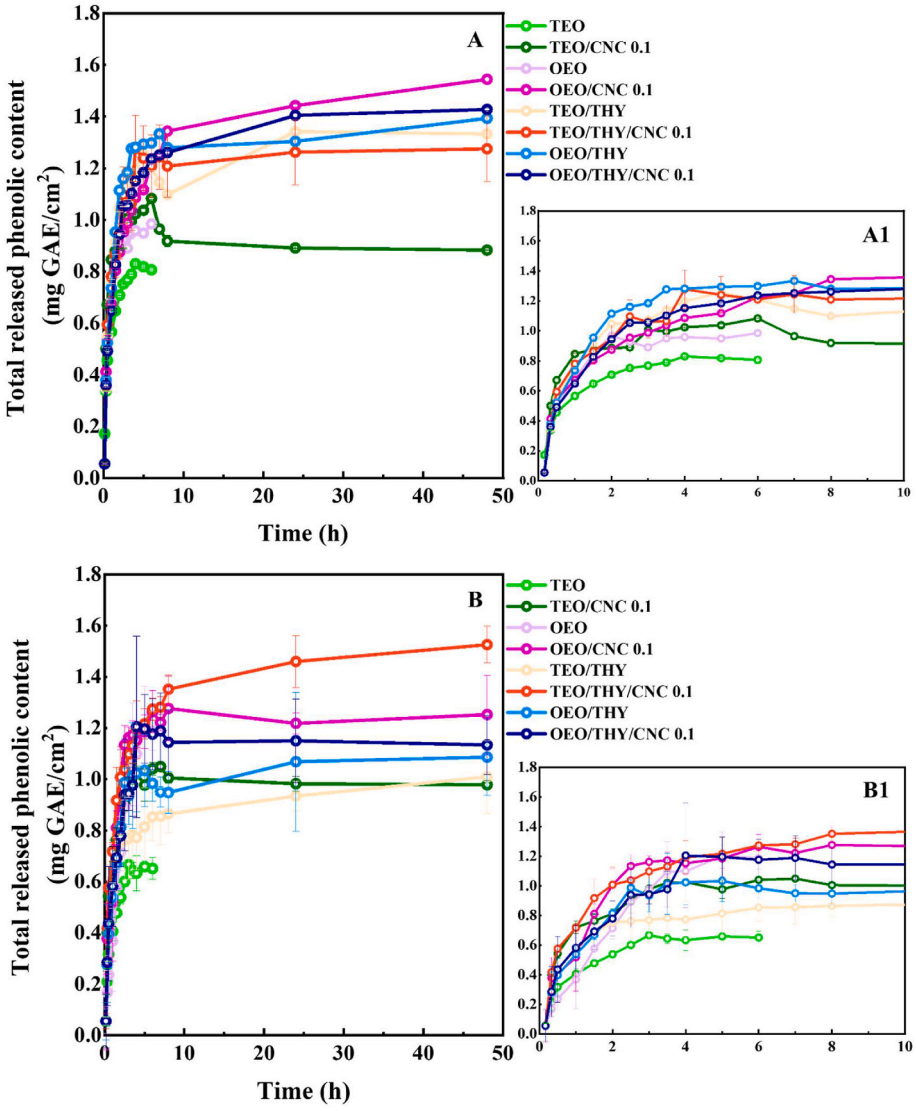

Fig. 7. The total released phenolic content of hydrocolloidal polymeric film systems over time at 4 (A) and 23 °C (B). Figures A1 and B1 are the zoom portions of figures A and B, respectively, during the first 10 h.

followed by the films incorporated with the combination of OEO EO/THY and TEO EO/THY while the lowest values were observed in TEO EO-added films. Generally, OEO EO-included films showed higher total phenolic content values. On the other hand, films including the complex of TEO EO-THY and OEO EO-THY showed significantly higher antioxidant activities than in their individually added films for both temperatures (Fig. 8). According to Mutlu-Ingok et al. (2021) OEO EO has higher carvacrol content while TEO EO includes a higher amount of THY when compared with each other. Besides, it has been reported that the combination of different EOs presented a synergistic effect giving higher biological activities than their sum of individual activities (Mutlu-Ingok et al., 2021). Thus, the results obtained for the films after being released into the medium agree with the studies reported for various films including EOs.

The relationship between the antioxidant activity and measured total phenolic content depending on the release time was plotted to understand the correlation between measures during the release test (Fig. 9). Pearson's correlation coefficients ranged between 83.8 – 98.0% and 89.7–97.8% for 4 and 23 °C (Table S3), respectively, showing a positive correlation.

3.7. Antimicrobial properties

This study aimed to assess the antimicrobial activity of active films by disk diffusion method against a wide range of microorganisms including both negative and positive bacteria, yeasts, and mold, and the results obtained are reported in Table 5.

Control films exhibited no inhibition zones on the growth of the tested microorganisms as control films cannot migrate and release the protonated glucosamine fractions of chitosan into the medium to inhibit microorganisms. In contrast, all films with EOs or EOs-THY complex with and without CNC showed higher antimicrobial activity. THY, as one of the major compounds of TEO EO, enhanced the antibacterial and antifungal activity in prepared films. It can be seen in Table 5 that TEO/THY or OEO/THY films which include the EOs-THY complex, presented the highest antimicrobial effect against the tested bacteria, fungi, and yeast in comparison with TEO or OEO films. Similar synergistic effects were recently described in detail by Sivaram et al. (2022) where TEO and OEO EOs were blended and enhanced microbial growth inhibition. These films showed the lowest cumulative release of the EOs-THY complex of around 21–25% and its major part remained in the films as in contact with microbes, which can be associated with the extended retention effect of the EOs-THY complex.

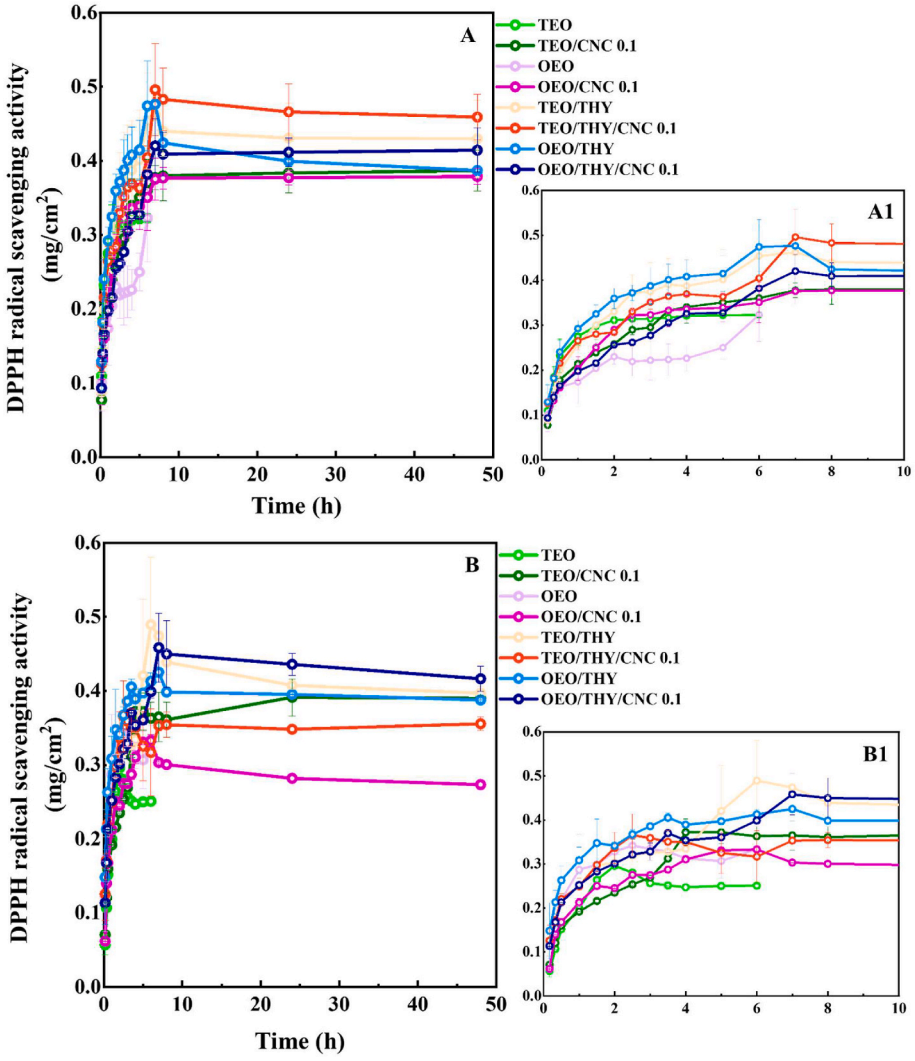

Fig. 8. DPPH scavenging activity profiles of hydrocolloidal polymeric film systems at 4 (A) and 23 °C (B). Figures A1 and B1 are the zoom portions of figures A and B, respectively, during the first 10 h.

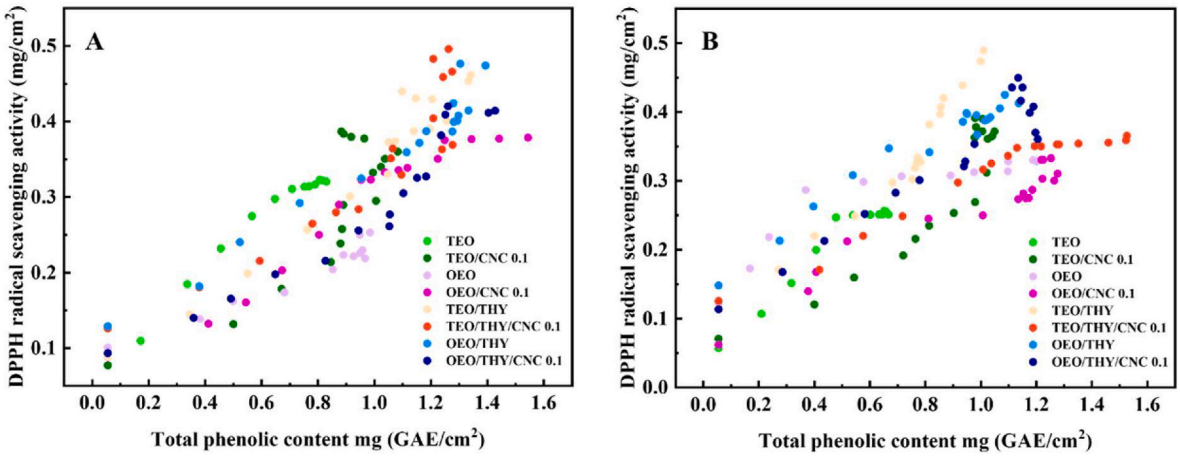

Fig. 9. The relationship between total phenolic content and antioxidant activity of hydrocolloidal polymeric film systems at 4 (A) and 23 °C (B).

In this study, CNC was proven to be excellent as a physical stabilizer in sustaining the films' mechanical integrity for a longer period, which means CNC can maintain EO-based films over a sustained period in contact with food. The addition of CNC 0.05% did not lead to a particular trend in films' antimicrobial activities while CNC 0.1% slightly restricted the activity compared to CNC-free films (Table 5 and Fig. 10). It was reported in Table 3 that CNC 0.1% accelerated the initial release rates of EOs from films in the buffer environment. However, the

Table 3
Initial release rates, total released amount, and Peleg's model kinetics.

Film composition				Initial release rate (%/h)[a]				Total released content (%)		Peleg's model kinetics[b]					
										4 °C			23 °C		
TEO (%)	OEO (%)	THY (%)	CNC (%)	4 °C	R^2	23 °C	R^2	4 °C	23 °C	$1/k_1$ (w/w %/h)	$1/k_2$ (g/g film)	R^2	$1/k_1$ (w/w %/h)	$1/k_2$ (g/g film)	R^2
2				42.50 ± 0.15^{aB}	0.99	41.60 ± 0.36^{aA}	0.99	57.49 ± 0.42^{aB}	58.40 ± 0.78^{aA}	51.27 ± 0.38^{cB}	38.88 ± 0.17^{aA}	0.96	55.02 ± 0.25^{bA}	39.53 ± 0.66^{aA}	0.94
2			0.1	49.66 ± 0.63^{aA}	0.99	44,67 ± 1.71^{aA}	0.99	51.62 ± 0.18^{bA}	60.23 ± 0.55^{bA}	104.61 ± 0.30^{aA}	34.92 ± 0.11^{bB}	0.82	79.20 ± 4.24^{aB}	40.50 ± 0.71^{aA}	0.95
	2			34.22 ± 0.02^{abB}	0.99	28.59 ± 0.12^{bcA}	0.99	42.31 ± 1.36^{cA}	42.37 ± 0.35^{cA}	48.21 ± 0.30^{dA}	27.97 ± 0.05^{cA}	0.95	28.11 ± 2.76^{eB}	29.58 ± 0.61^{bA}	0.97
	2		0.1	36.40 ± 0.14^{abA}	0.99	31.21 ± 0.01^{bA}	0.99	42.83 ± 0.22^{cA}	42.85 ± 0.80^{cA}	73.14 ± 0.76^{bA}	28.87 ± 0.19^{cA}	0.99	35.94 ± 0.17^{cdB}	24.75 ± 0.36^{cB}	0.90
2		2		16.92 ± 0.17^{abB}	0.99	17.61 ± 0.30^{cA}	0.99	25.06 ± 0.30^{dB}	26.01 ± 0.25^{dA}	20.28 ± 0.17^{fB}	17.50 ± 0.70^{dA}	0.92	28.74 ± 0.08^{deA}	17.47 ± 0.11^{deA}	0.89
2		2	0.1	18.99 ± 0.13^{abB}	0.99	18.41 ± 0.15^{bA}	0.99	24.28 ± 0.66^{dB}	25.70 ± 0.19^{dA}	20.88 ± 0.17^{fA}	16.66 ± 0.49^{deA}	0.91	17.34 ± 0.93^{fB}	18.18 ± 0.23^{dA}	0.90
	2	2		18.98 ± 0.08^{bB}	0.99	19.74 ± 0.08^{dA}	0.99	21.94 ± 0.33^{eA}	22.04 ± 0.74^{eA}	29.01 ± 1.40^{eA}	14.88 ± 0.18^{fA}	0.92	20.40 ± 0.85^{fB}	15.26 ± 0.28^{fA}	0.88
	2	2	0.1	19.50 ± 0.01^{bB}	0.99	23.01 ± 0.30^{dA}	0.99	23.29 ± 0.53^{eB}	23.34 ± 0.26^{eA}	23.04 ± 1.36^{fB}	15.86 ± 0.20^{efA}	0.99	43.11 ± 0.13^{cA}	15.85 ± 0.21^{efA}	0.90

Means with different lowercase letters indicate significant differences within a column **(between samples)** based on Tukey's test ($p < 0.05$). Means with different uppercase letters indicate significant differences within a row **(between temperature)** based on Tukey's test ($p < 0.05$).
Results mean ± standard deviation (n = 3).
[a] A period of 1 h was selected due to the data used in best fit.
[b] k_1 is related to the release rate at the beginning of the process and k_2 is related to the asymptotic value, which is obtained from the inverse of the amount of EO released at the equilibrium.

Table 4
Total phenolic content and antioxidant activity of hydrocolloidal polymeric film systems.

Film composition				Total released phenolic content (mg GAE/cm^2)[a]		Antioxidant activity (mg/cm^2)[a]	
TEO (%)	OEO (%)	THY (%)	CNC (%)	4 °C	23 °C	4 °C	23 °C
2				0.906 ± 0.002^{dA}	0.856 ± 0.022^{bB}	0.343 ± 0.008^{abA}	0.296 ± 0.006^{dB}
2			0.1	0.883 ± 0.002^{eB}	1.006 ± 0.022^{abA}	0.387 ± 0.028^{abA}	0.390 ± 0.012^{bA}
	2			1.152 ± 0.012^{cB}	1.222 ± 0.070^{abA}	0.314 ± 0.002^{bB}	0.342 ± 0.039^{bcA}
	2		0.1	1.544 ± 0.013^{aA}	1.224 ± 0.035^{abB}	0.379 ± 0.011^{abA}	0.331 ± 0.003^{dB}
2		2		1.333 ± 0.002^{bA}	0.999 ± 0.169^{abB}	0.454 ± 0.052^{abA}	0.474 ± 0.019^{aA}
2		2	0.1	1.275 ± 0.128^{bB}	1.523 ± 0.032^{aA}	0.466 ± 0.031^{aA}	0.359 ± 0.029^{bcB}
	2	2		1.393 ± 0.011^{abA}	1.136 ± 0.170^{abB}	0.474 ± 0.001^{aA}	0.413 ± 0.001^{bB}
	2	2	0.1	1.427 ± 0.006^{abA}	1.112 ± 0.110^{abB}	0.414 ± 0.030^{abB}	0.436 ± 0.010^{abA}

Lowercase letters and uppercase letters indicate significant differences within a column **(between samples)** and a row **(between temperature),** respectively based on Tukey's test ($p < 0.05$).
Results mean ± standard deviation ($n = 3$).
[a] The amounts are equilibrium values.

Table 5
Antimicrobial activity of hydrocolloidal polymeric film systems performed by disk diffusion method (disk diameter 9 mm).

Films	Inhibition zone (mm)				
	S. aureus (Gram positive bacteria)	*E. coli (Gram negative bacteria)*	*C. albicans (Yeast)*	*C. parapsilosis (Yeast)*	*A.brasiliensis (Fungi)*
Control	9.0 ± 0.0^{a}	9.0 ± 0.0^{a}	9.0 ± 0.0^{a}	9.0 ± 0.0^{a}	9.0 ± 0.0^{a}
TEO	19.0 ± 1.4^{d}	14.0 ± 0.0^{d}	10.8 ± 0.4^{c}	11.0 ± 0.0^{c}	14.7 ± 1.9^{c}
TEO/CNC 0.05	18.2 ± 0.4^{d}	12.5 ± 0.5^{c}	11.5 ± 0.5^{c}	10.5 ± 0.5^{c}	18.2 ± 1.9^{d}
TEO/CNC 0.1	14.5 ± 0.5^{b}	11.0 ± 0.0^{b}	10.0 ± 0.6^{b}	9.3 ± 0.3^{ab}	11.5 ± 1.4^{b}
OEO	18.0 ± 0.0^{d}	15.0 ± 0.0^{d}	11.5 ± 0.5^{c}	10.5 ± 0.8^{c}	22.0 ± 1.3^{e}
OEO/CNC 0.05	17.7 ± 0.5^{c}	12.8 ± 0.4^{c}	11.2 ± 0.4^{c}	10.5 ± 0.5^{c}	22.3 ± 1.2^{e}
OEO/CNC 0.1	14.7 ± 0.5^{b}	11.8 ± 0.4^{bc}	10.5 ± 0.8^{bc}	9.7 ± 0.3^{b}	16.2 ± 2.9^{cd}
TEO/THY	21.3 ± 1.2^{ef}	15.7 ± 1.6^{d}	13.3 ± 1.9^{e}	12.0 ± 0.0^{d}	25.8 ± 6.6^{ef}
TEO/THY/CNC 0.05	21.2 ± 0.8^{f}	13.3 ± 0.5^{c}	13.8 ± 1.6^{def}	10.8 ± 1.1^{cd}	23.3 ± 4.0^{ef}
TEO/THY/CNC 0.1	17.3 ± 0.5^{c}	12.8 ± 0.4^{c}	11.0 ± 0.0^{c}	9.9 ± 0.9^{bc}	18.0 ± 0.9^{d}
OEO/THY	20.8 ± 0.8^{e}	15.0 ± 0.6^{d}	15.5 ± 2.3^{def}	12.7 ± 0.5^{d}	29.2 ± 4.5^{f}
OEO/THY/CNC 0.05	22.3 ± 0.8^{f}	15.5 ± 0.5^{d}	18.3 ± 2.9^{f}	15.3 ± 0.5^{e}	14.3 ± 4.7^{cd}
OEO/THY/CNC 0.1	19.0 ± 1.4^{cde}	12.8 ± 0.4^{c}	12.0 ± 0.9^{cde}	11.0 ± 0.0^{c}	17.3 ± 1.6^{d}

Different letters in the same column are significantly different based on Tukey's test ($p < 0.05$).
Results mean ± standard deviation ($n = 3$).

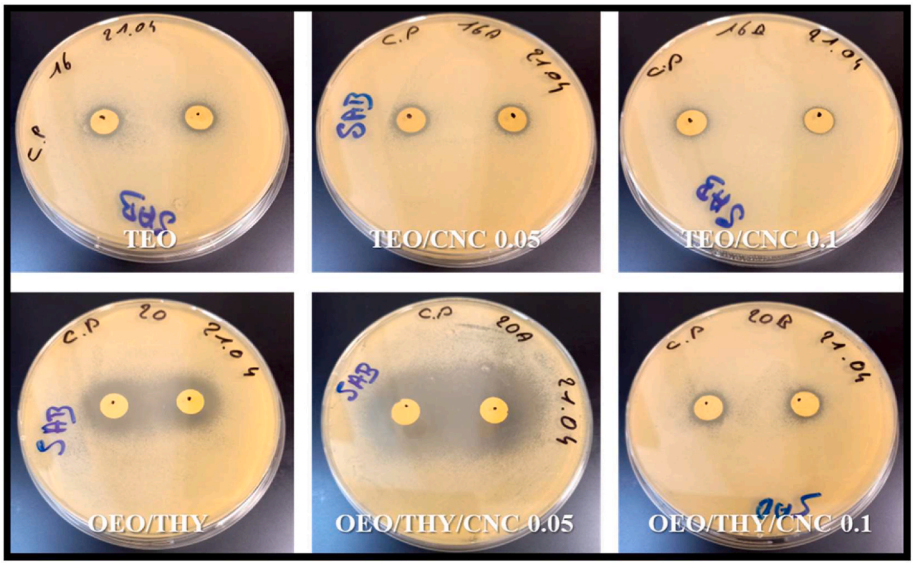

Fig. 10. The effect of CNC concentration on the antimicrobial effectiveness of films against *C. parapsilosis*.

agar medium used for antimicrobial testing was not the same as the buffer medium, and release depends on contact conditions and medium characteristics, e.g. the pH and temperature. Therefore, EOs and EOs/THY in contact with the agar medium might have followed different release patterns than the buffer and the optimal quantity to inhibit microbial activity might not have been maintained on the agar surface.

The antimicrobial activity of EOs generally initiates with their ability to penetrate the cell walls of the microbes. As reported in Table 5, the inhibition zones of films against Gram-negative bacteria *E. coli* and yeasts *C. albicans* and *C. parapsilosis* were smaller than Gram-positive bacteria *S. aureus* and fungi *A. brasiliensis*, indicating their higher resistivity to EOs and THY. The cell wall of Gram-negative bacteria is more complex. This complexity arises from the presence of the outer membrane in Gram-negative bacteria's cell structure, composed of phospholipids, lipopolysaccharides, and lipoproteins, which differ from Gram-positive bacteria. Such structure of Gram-negative bacteria limits the diffusion of hydrophobic EO compounds toward the cell wall of bacteria, resulting in reduced antimicrobial activity (Nazzaro et al., 2013). Likewise, the cell walls of yeasts *C. albicans* and *C. parapsilosis* are complex with the structure composed of four main polysaccharides arranged in two well-defined layers: the outermost layer with glycoproteins and mannans, and the inner layer with chitin and glucan (Estrada-Mata et al., 2016).

4. Conclusion

Bio-based active delivery systems are becoming increasingly important for sustainable food packaging as they can reduce both food and packaging waste by extending shelf-life. Hydrocolloids, like zein and chitosan, can be loaded with antimicrobial or antioxidant compounds to make them bioactive and used as an active packaging layer in primary contact with food. However, such systems mostly suffer from rapid hydrolysis upon contact with food, in particular when the moisture content is high or moderate, which eventually leads to undesirable release behavior of active compounds. This study demonstrated that providing structural reinforcement with CNC increased the hydrolytic resistance of bioactive hydrocolloidal film systems and enhanced release behavior. Active compounds, when blended, exhibited synergistic effects against hydrolysis like CNC-added films, however, the high amount of EOs content may be considered undesirable for organoleptic characteristics. This approach can be extended to other food model systems that mimic the composition of food complex matrices such as acidic and oily food to investigate its tailorability and validity.

CRediT authorship contribution statement

Lucie Pavlatkova: Writing – original draft, Methodology, Investigation, Formal analysis. **Ece Sogut:** Writing – original draft, Validation, Software, Methodology, Investigation, Formal analysis. **Jana Sedlarikova:** Writing – review & editing, Validation, Supervision, Methodology, Formal analysis, Conceptualization. **Pavel Pleva:** Visualization, Software, Methodology, Investigation. **Lucas Petit:** Methodology, Investigation. **Milan Masar:** Methodology, Investigation. **Petra Peer:** Writing – review & editing, Investigation. **Magda Janalikova:** Writing – review & editing, Supervision, Investigation, Funding acquisition, Conceptualization. **Ilke Uysal-Unalan:** Writing – review & editing, Writing – original draft, Validation, Supervision, Resources, Project administration, Methodology, Investigation, Funding acquisition, Conceptualization.

Funding

The authors acknowledge the support given by the Internal Grant Agency of Tomas Bata University in Zlín (project No. IGA/FT/2022/006).

Declaration of competing interest

The authors declare that they have no known competing financial interests or personal relationships that could have appeared to influence the work reported in this paper.

Acknowledgments

Lucie Pavlatkova would like to thank COST Action Circul-a-bility (CA19124 - Rethinking Packaging for Circular and Sustainable Food Supply Chains of The Future), supported by COST (European Cooperation in Science and Technology). The authors would like to acknowledge Dr. Thomas William Seviour from the Department of Biological and Chemical Engineering at Aarhus University for his comments and suggestions on the manuscript. Some of the data were generated through accessing research infrastructure at Aarhus University, including FOODHAY (Food and Health Open Innovation Laboratory, Danish Roadmap for Research Infrastructure).

Appendix A. Supplementary data

Supplementary data to this article can be found online at https://doi.org/10.1016/j.foodhyd.2025.111316.

Data availability

Data will be made available on request.

References

Alves, J. S., Dos Reis, K. C., Menezes, E. G. T., Pereira, F. V., & Pereira, J. (2015). Effect of cellulose nanocrystals and gelatin in corn starch plasticized films. *Carbohydrate Polymers, 115*, 215–222.

Aranaz, I., Alcántara, A. R., Civera, M. C., Arias, C., Elorza, B., Heras Caballero, A., et al. (2021). Chitosan: An overview of its properties and applications. *Polymers, 13*(19), 3256.

Asgher, M., Qamar, S. A., Bilal, M., & Iqbal, H. M. (2020). Bio-based active food packaging materials: Sustainable alternative to conventional petrochemical-based packaging materials. *Food Research International, 137*, Article 109625.

Bassolé, I. H. N., & Juliani, H. R. (2012). Essential oils in combination and their antimicrobial properties. In *Molecules* (Vol. 17, pp. 3989–4006). MDPI. https://doi.org/10.3390/molecules17043989, 4.

Cazón, P., Morales-Sanchez, E., Velazquez, G., & Vázquez, M. (2022). Measurement of the water vapor permeability of chitosan films: A laboratory experiment on food packaging materials. *Journal of Chemical Education, 99*(6), 2403–2408.

Charles, A. P. R., Mu, R., Jin, T. Z., Li, D., Pan, Z., Rakshit, S., … Wu, Y. (2022). Application of yellow mustard mucilage and starch in nanoencapsulation of thymol and carvacrol by emulsion electrospray. *Carbohydrate Polymers, 298*, Article 120148.

Chen, Q., Auras, R., & Uysal-Unalan, I. (2022). Role of stereocomplex in advancing mass transport and thermomechanical properties of polylactide. *Green Chemistry, 24*(9), 3416–3432.

Chen, Q., Sogut, E., Auras, R., Kirkensgaard, J. J. K., & Uysal-Unalan, I. (2024). Hydrolysis of biobased stereocomplex polylactide: Polymorphism dependent crystals degradation and evolution of three-phase crystalline composition. *Applied Materials Today, 38*, Article 102226.

Chen, H., Wang, J., Cheng, Y., Wang, C., Liu, H., Bian, H., et al. (2019). Application of protein-based films and coatings for food packaging: A review. *Polymers, 11*(12). https://doi.org/10.3390/polym11122039

Chen, X., Xiao, J., Cai, J., & Liu, H. (2020). Phase separation behavior in zein-gelatin composite film and its modulation effects on retention and release of multiple bioactive compounds. *Food Hydrocolloids, 109*(June), Article 106105. https://doi.org/10.1016/j.foodhyd.2020.106105

Chi, K., & Catchmark, J. M. (2018). Improved eco-friendly barrier materials based on crystalline nanocellulose/chitosan/carboxymethyl cellulose polyelectrolyte complexes. *Food Hydrocolloids, 80*, 195–205.

Coppola, D., Lauritano, C., Palma Esposito, F., Riccio, G., Rizzo, C., & de Pascale, D. (2021). Fish waste: From problem to valuable resource. *Marine Drugs, 19*(2), 116.

Crowe, K. M. (2013). Designing functional foods with bioactive polyphenols: Highlighting lessons learned from original plant matrices. *J Hum Nutr Food Sci, 1*(3), 1018.

Cruz, R. M., Krauter, V., Krauter, S., Agriopoulou, S., Weinrich, R., Herbes, C., … Varzakas, T. (2022). Bioplastics for food packaging: Environmental impact, trends and regulatory aspects. *Foods, 11*(19), 3087.

de Oliveira Filho, J., de Deus, I., Valadares, A., Fernandes, C., Estevam, E., & Egea, M. (2020). Chitosan film with citrus limonia essential oil: Physical and morphological properties and antibacterial activity. *Colloids and Interfaces, 4*(issue 2). https://doi.org/10.3390/colloids4020018 [Online].

Deng, L., Kang, X., Liu, Y., Feng, F., & Zhang, H. (2018). Characterization of gelatin/zein films fabricated by electrospinning vs solvent casting. *Food Hydrocolloids, 74*, 324–332.

Deng, L., Li, Y., Feng, F., Wu, D., & Zhang, H. (2019). Encapsulation of allopurinol by glucose cross-linked gelatin/zein nanofibers: Characterization and release behavior. *Food Hydrocolloids, 94*, 574–584.

Dickinson, E. (2017). Biopolymer-based particles as stabilizing agents for emulsions and foams. *Food Hydrocolloids, 68*, 219–231.

Eranda, D. H. U., Chaijan, M., Uysal-Unalan, I., Panpipat, W., Naik, A. S., Dib, A. L., … Gagaoua, M. (2024). Biopreservation of pre-processed fresh fish by bio-based coating. *Food Bioscience*, Article 103696.

Estrada-Mata, E., Navarro-Arias, M. J., Pérez-García, L. A., Mellado-Mojica, E., López, M. G., Csonka, K., … Mora-Montes, H. M. (2016). Members of the Candida parapsilosis complex and Candida albicans are differentially recognized by human peripheral blood mononuclear cells. *Frontiers in Microbiology, 6*, 1527.

European Union, 2024. https://www.europarl.europa.eu/news/en/agenda/briefing/2024-04-22/1/final-vote-on-new-eu-rules-for-sustainable-packaging.

Fernandes, S. C., Oliveira, L., Freire, C. S., Silvestre, A. J., Neto, C. P., Gandini, A., et al. (2009). Novel transparent nanocomposite films based on chitosan and bacterial cellulose. *Green Chemistry, 11*(12), 2023–2029.

Fernández-Pan, I., Maté, J. I., Gardrat, C., & Coma, V. (2015). Effect of chitosan molecular weight on the antimicrobial activity and release rate of carvacrol-enriched films. *Food Hydrocolloids, 51*, 60–68. https://doi.org/10.1016/j.foodhyd.2015.04.033

Gagaoua, M., Bhattacharya, T., Lamri, M., Oz, F., Dib, A. L., Oz, E., … Tomasevic, I. (2021). Green coating polymers in meat preservation. *Coatings, 11*(11), 1379.

Ghadermazi, R., Hamdipour, S., Sadeghi, K., Ghadermazi, R., & Khosrowshahi Asl, A. (2019). Effect of various additives on the properties of the films and coatings derived from hydroxypropyl methylcellulose—A review. *Food Science & Nutrition, 7*(11), 3363–3377.

Giotopoulou, I., Stamatis, H., & Barkoula, N. M. (2024). Encapsulation of thymol in ethyl cellulose-based microspheres and evaluation of its sustained release for food applications. *Polymers, 16*(23), 3396.

Giteru, S. G., Ali, M. A., & Oey, I. (2019). Solvent strength and biopolymer blending effects on physicochemical properties of zein-chitosan-polyvinyl alcohol composite films. *Food Hydrocolloids, 87*, 270–286.

González-Reza, R. M., Hernández-Sánchez, H., Quintanar-Guerrero, D., Alamilla-Beltrán, L., Cruz-Narváez, Y., & Zambrano-Zaragoza, M. L. (2021). Synthesis, controlled release, and stability on storage of chitosan-thyme essential oil nanocapsules for food applications. *Gels, 7*(4), 212.

Granata, G., Stracquadanio, S., Leonardi, M., Napoli, E., Malandrino, G., Cafiso, V., … Geraci, C. (2021). Oregano and thyme essential oils encapsulated in chitosan nanoparticles as effective antimicrobial agents against foodborne pathogens. *Molecules, 26*(13), 4055.

Gupta, K. C., Majeti, N., & Kumar, V. R. (2001). pH dependent hydrolysis and drug release behavior of chitosan/poly (ethylene glycol) polymer network microspheres. *Journal of Materials Science: Materials in Medicine, 12*(9), 753.

Gurpreet, K., & Singh, S. K. (2018). Review of nanoemulsion formulation and characterization techniques. *Indian Journal of Pharmaceutical Sciences, 80*(5), 781–789.

Hamedi, S., Mahmoodi-Barmesi, M., Kermanian, H., Ramezani, O., & Razmpour, Z. (2024). Investigation of physicochemical and biological properties of bacterial cellulose & zein-reinforced edible nanocomposites based on flaxseed mucilage containing Origanum vulgare L. essential oil. *International Journal of Biological Macromolecules, 254*, Article 127733.

Iñiguez-Franco, F., Auras, R., Ahmed, J., Selke, S., Rubino, M., Dolan, K., et al. (2018). Control of hydrolytic degradation of Poly (lactic acid) by incorporation of chain extender: From bulk to surface erosion. *Polymer Testing, 67*, 190–196.

Kashiri, M., Cerisuelo, J. P., Domínguez, I., López-Carballo, G., Muriel-Gallet, V., Gavara, R., et al. (2017). Zein films and coatings as carriers and release systems of Zataria multiflora Boiss. essential oil for antimicrobial food packaging. *Food Hydrocolloids, 70*, 260–268. https://doi.org/10.1016/j.foodhyd.2017.02.021

Kunam, P. K., Ramakanth, D., Akhila, K., & Gaikwad, K. K. (2022). Bio-based materials for barrier coatings on paper packaging. *Biomass Conversion and Biorefinery*, 1–16.

Lee, M. H., Kim, S. Y., & Park, H. J. (2018). Effect of halloysite nanoclay on the physical, mechanical, and antioxidant properties of chitosan films incorporated with clove essential oil. *Food Hydrocolloids, 84*, 58–67.

Li, Z., Jiang, X., Huang, H., Liu, A., Liu, H., Abid, N., et al. (2022). Chitosan/zein films incorporated with essential oil nanoparticles and nanoemulsions: Similarities and differences. *International Journal of Biological Macromolecules, 208*, 983–994.

Lian, H., Peng, Y., Shi, J., & Wang, Q. (2019). Effect of emulsifier hydrophilic-lipophilic balance (HLB) on the release of thyme essential oil from chitosan films. *Food Hydrocolloids, 97*, Article 105213.

Liu, J., Song, F., Chen, R., Deng, G., Chao, Y., Yang, Z., … Hu, Y. (2022). Effect of cellulose nanocrystal-stabilized cinnamon essential oil Pickering emulsions on structure and properties of chitosan composite films. *Carbohydrate Polymers, 275*, Article 118704.

Manzanarez-López, F., Soto-Valdez, H., Auras, R., & Peralta, E. (2011). Release of α-Tocopherol from Poly(lactic acid) films, and its effect on the oxidative stability of soybean oil. *Journal of Food Engineering, 104*(issue 4), 508–517 [Online].

Mathew, S., Brahmakumar, M., & Abraham, T. E. (2006). Microstructural imaging and characterization of the mechanical, chemical, thermal, and swelling properties of starch–chitosan blend films. *Biopolymers: Original Research on Biomolecules, 82*(2), 176–187.

Mendes, J. F., Norcino, L. B., Martins, H. H. A., Manrich, A., Otoni, C. G., Carvalho, E. E. N., … Mattoso, L. H. C. (2020). Correlating emulsion characteristics with the properties of active starch films loaded with lemongrass essential oil. *Food Hydrocolloids, 100*, Article 105428.

Mortier, C., Costa, D. C. S., Oliveira, M. B., Haugen, H. J., Lyngstadaas, S. P., Blaker, J. J., et al. (2022). Advanced hydrogels based on natural macromolecules: Chemical routes to achieve mechanical versatility. *Materials Today Chemistry, 26*, Article 101222.

Mutlu-Ingok, A., Catalkaya, G., Capanoglu, E., & Karbancioglu-Guler, F. (2021). Antioxidant and antimicrobial activities of fennel, ginger, oregano and thyme essential oils. *Food Frontiers, 2*(4), 508–518.

Nazzaro, F., Fratianni, F., De Martino, L., Coppola, R., & De Feo, V. (2013). Effect of essential oils on pathogenic bacteria. *Pharmaceuticals, 6*(12), 1451–1474.

Nguyen, L. H., Naficy, S., Chandrawati, R., & Dehghani, F. (2019). Nanocellulose for sensing applications. *Advanced Materials Interfaces, 6*(18), Article 1900424.

Pavlátková, L., Sedlaříková, J., Pleva, P., Peer, P., Uysal-Unalan, I., & Janalíková, M. (2022). Bioactive chitosan/zein systems loaded with essential oils for food-packaging applications. *Journal of the Science of Food and Agriculture*.

Peleg, M. (1988). An empirical model for the description of moisture sorption curves. *Journal of Food Science, 53*(4), 1216–1217.

Perumal, A., Nambiar, R., Moses, J., & Anandharamakrishnan, C. (2022). Nanocellulose: Recent trends and applications in the food industry [Online]. *Food Hydrocolloids, 127* (107484), 1–23. https://doi.org/10.1016/j.foodhyd.2022.107484

Pires, J., Paula, C. D. D., Souza, V. G. L., Fernando, A. L., & Coelhoso, I. (2021). Understanding the barrier and mechanical behavior of different nanofillers in chitosan films for food packaging. *Polymers, 13*(5), 721.

Ramos, M., Beltrán Sanahuja, A., Valdés, A., Peltzer, M. A., Jimenez, A., Garrigós, M. D. C., et al. (2013). *Active packaging for fresh food based on the release of carvacrol and thymol*.

Reichert, C. L., Bugnicourt, E., Coltelli, M. B., Cinelli, P., Lazzeri, A., Canesi, I., … Schmid, M. (2020). Bio-based packaging: Materials, modifications, industrial applications and sustainability. *Polymers, 12*(7), 1558.

Salari, M., Khiabani, M. S., Mokarram, R. R., Ghanbarzadeh, B., & Kafil, H. S. (2018). Development and evaluation of chitosan based active nanocomposite films containing bacterial cellulose nanocrystals and silver nanoparticles. *Food Hydrocolloids, 84*, 414–423.

Sampaio, A. P. C., Müller-Carneiro, J., Pereira, A. L. S., de Freitas Rosa, M., Mattos, A. L. A., de Azeredo, H. M. C., … de Figueirêdo, M. C. B. (2023). Ecodesign of bio-based films for food packaging: Challenges and recommendations. *Environmental Development*, Article 100926.

Santos, V. P., Marques, N. S., Maia, P. C., Lima, M. A. B. D., Franco, L. D. O., & Campos-Takaki, G. M. D. (2020). Seafood waste as attractive source of chitin and chitosan production and their applications. *International Journal of Molecular Sciences, 21*(12), 4290.

Schmidt, J., Grau, L., Auer, M., Maletz, R., & Woidasky, J. (2022). Multilayer packaging in a circular economy. *Polymers, 14*(9), 1825.

Schulz, H., Quilitzsch, R., & Krüger, H. (2003). Rapid evaluation and quantitative analysis of thyme, origano and chamomile essential oils by ATR-IR and NIR spectroscopy. *Journal of Molecular Structure, 661*, 299–306.

Sedlaříková, J., Doležalová, M., Egner, P., Pavlačková, J., Krejčí, J., Rudolf, O., et al. (2017). Effect of oregano and marjoram essential oils on the physical and antimicrobial properties of chitosan based systems [online]. *International Journal Of Polymer Science, 2017*, 1–12. https://doi.org/10.1155/2017/2593863

Sedlarikova, J., Janalikova, M., Peer, P., Pavlatkova, L., Minarik, A., & Pleva, P. (2021). Zein-based films containing monolaurin/eugenol or essential oils with potential for bioactive packaging application. *International Journal of Molecular Sciences, 23*(1), 384.

Sedlaříková, J., Janalíková, M., Rudolf, O., Pavlačková, J., Egner, P., Peer, et al. (2019). Chitosan/thyme oil systems as affected by stabilizing agent: Physical and antimicrobial properties. *Coatings, 9*, 1–18.

Shukla, R., & Cheryan, M. (2001). Zein: The industrial protein from corn. *Industrial Crops and Products, 13*(3), 171–192.

Singleton, V. L., & Rossi, J. A. (1965). Colorimetry of total phenolics with phosphomolybdic-phosphotungstic acid reagents. *American Journal of Enology and Viticulture, 16*(3), 144–158.

Sivaram, S., Somanathan, H., Kumaresan, S. M., & Muthuraman, M. S. (2022). The beneficial role of plant based thymol in food packaging application: A comprehensive review. *Applied Food Research, 2*(2). https://doi.org/10.1016/j.afres.2022.100214 [Online].

Soofi, M., Alizadeh, A., Hamishehkar, H., Almasi, H., & Roufegarinejad, L. (2021). Preparation of nanobiocomposite film based on lemon waste containing cellulose nanofiber and savory essential oil: A new biodegradable active packaging system. *International Journal of Biological Macromolecules, 169*, 352–361.

Souza, A. G. D., Ferreira, R. R., Aguilar, E. S. F., Zanata, L., & Rosa, D. D. S. (2021). Cinnamon essential oil nanocellulose-based pickering emulsions: Processing parameters effect on their formation, stabilization, and antimicrobial activity. *Polysaccharides, 2*(3), 608–625.

Sun, C., Cao, J., Wang, Y., Huang, L., Chen, J., Wu, J., … Sun, C. (2022). Preparation and characterization of pectin-based edible coating agent encapsulating carvacrol/HPβCD inclusion complex for inhibiting fungi. *Food Hydrocolloids, 125*, Article 107374.

Sun, Q., Sheng, J., & Yang, R. (2021). Controllable biodegradation and drug release behavior of chitosan-graft-poly (D, L-lactic acid) synthesized by an efficient method. *Polymer Degradation and Stability, 186*, Article 109458.

Tyagi, P., Salem, K. S., Hubbe, M. A., & Pal, L. (2021). Advances in barrier coatings and film technologies for achieving sustainable packaging of food products–a review. *Trends in Food Science & Technology, 115*, 461–485.

Ulloa-Saavedra, A., García-Betanzos, C., Zambrano-Zaragoza, M., Quintanar-Guerrero, D., Mendoza-Elvira, S., & Velasco-Bejarano, B. (2022). Recent developments and applications of nanosystems in the preservation of meat and meat products. In *Foods* (Vol. 11, p. 2150). MDPI. https://doi.org/10.3390/foods11142150, 14.

Uysal-Unalan, I., Sogut, E., Realini, C. E., Cakmak, H., Oz, E., Espinosa, E., … Corredig, M. (2024). Bioplastic packaging for fresh meat and fish: Current status and future direction on mitigating food and packaging waste. *Trends in Food Science & Technology*, Article 104660.

Vahedikia, N., Garavand, F., Tajeddin, B., Cacciotti, I., Jafari, S. M., Omidi, T., et al. (2019). Biodegradable zein film composites reinforced with chitosan nanoparticles and cinnamon essential oil: Physical, mechanical, structural and antimicrobial attributes. *Colloids and Surfaces B: Biointerfaces, 177*, 25–32.

Vieira, A. C., Guedes, R. M., & Tita, V. (2013). Considerations for the design of polymeric biodegradable products. *Journal of Polymer Engineering, 33*(4), 293–302.

Villegas, C., Arrieta, M. P., Rojas, A., Torres, A., Faba, S., Toledo, M. J., … Valenzuela, X. (2019). PLA/organoclay bionanocomposites impregnated with thymol and cinnamaldehyde by supercritical impregnation for active and sustainable food packaging. *Composites Part B: Engineering, 176*, Article 107336.

Wang, K., Wu, K., Xiao, M., Kuang, Y., Corke, H., Ni, X., et al. (2017). Structural characterization and properties of konjac glucomannan and zein blend films. *International Journal of Biological Macromolecules, 105*, 1096–1104.

Wardhono, E. Y., Pinem, M. P., Kustiningsih, I., Agustina, S., Oudet, F., Lefebvre, C., … Guénin, E. (2019). Cellulose nanocrystals to improve stability and functional properties of emulsified film based on chitosan nanoparticles and beeswax. *Nanomaterials, 9*(12), 1707.

Xue, F., Zhao, M., Liu, X., Chu, R., Qiao, Z., Li, C., et al. (2021). Physicochemical properties of chitosan/zein/essential oil emulsion-based active films functionalized by polyphenols. *Future Foods, 3*, Article 100033.

Yakoubi, S., Bourgou, S., Mahfoudhi, N., Hammami, M., Khammassi, S., Horchani-Naifer, K., et al. (2020). Oil-in-water emulsion formulation of cumin/carvi essential oils combination with enhanced antioxidant and antibacterial potentials. *Journal of Essential Oil Research, 32*(6), 536–544. https://doi.org/10.1080/10412905.2020.1829510

Yang, W., Fortunati, E., Dominici, F., Giovanale, G., Mazzaglia, A., Balestra, G. M., … Puglia, D. (2016). Effect of cellulose and lignin on disintegration, antimicrobial and antioxidant properties of PLA active films. *International Journal of Biological Macromolecules, 89*, 360–368.

Yuan, X., Wang, Y., Cai, D., Zheng, M., Xiu, L., & Liu, J. (2016). Optimization by response surface methodology of film-forming properties of whey protein of glycosylation modifications at dry-heating condition. *Journal of Chinese Institute of Food Science and Technology, 16*(7), 105–112.

Zhang, X., Ismail, B. B., Cheng, H., Jin, T. Z., Qian, M., Arabi, S. A., … Guo, M. (2021). Emerging chitosan-essential oil films and coatings for food preservation-A review of advances and applications. *Carbohydrate Polymers, 273*, Article 118616.

Zhang, L., Li, K., Yu, D., Regenstein, J. M., Dong, J., Chen, W., et al. (2022). Chitosan/zein bilayer films with one-way water barrier characteristic: Physical, structural and thermal properties. *International Journal of Biological Macromolecules, 200*, 378–387.

Zhang, L., Liu, Z., Wang, X., Dong, S., Sun, Y., & Zhao, Z. (2019). The properties of chitosan/zein blend film and effect of film on quality of mushroom (Agaricus bisporus). *Postharvest Biology and Technology, 155*, 47–56.